Meteoritics & Planetary Science 40, Nr 7, 989–1014 (2005)
Abstract available online at http://meteoritics.org

"New" lunar meteorites: Impact melt and regolith breccias and large-scale heterogeneities of the upper lunar crust

Paul H. WARREN*, Finn ULFF-MØLLER, and Gregory W. KALLEMEYN

Institute of Geophysics, University of California—Los Angeles, Los Angeles, California 90095–1567, USA
*Corresponding author. E-mail: pwarren@ucla.edu

(Received 06 May 2002; revision accepted 24 April 2005)

Abstract–We have analyzed nine highland lunar meteorites (lunaites) using mainly INAA. Several of these rocks are difficult to classify. Dhofar 081 is basically a fragmental breccia, but much of its groundmass features a glassy-fluidized texture that is indicative of localized shock melting. Also, much of the matrix glass is swirly-brown, suggesting a possible regolith derivation. We interpret Dar al Gani (DaG) 400 as an extremely immature regolith breccia consisting mainly of impact-melt breccia clasts; we interpret Dhofar 026 as an unusually complex anorthositic impact-melt breccia with scattered ovoid globules that formed as clasts of mafic, subophitic impact melt. The presence of mafic crystalline globules in a lunar material, even one so clearly impact-heated, suggests that it may have originated as a regolith. Our new data and a synthesis of literature data suggest a contrast in Al_2O_3-incompatible element systematics between impact melts from the central nearside highlands, where Apollo sampling occurred, and those from the general highland surface of the Moon. Impact melts from the general highland surface tend to have systematically lower incompatible element concentration at any given Al_2O_3 concentration than those from Apollo 16. In the case of Dhofar 026, both the bulk rock and a comparatively Al-poor composition (14 wt% Al_2O_3, 7 µg/g Sm) extrapolated for the globules, manifest incompatible element contents well below the Apollo 16 trend. Impact melts from Luna 20 (57°E) distribute more along the general highland trend than along the Apollo 16 trend. Siderophile elements also show a distinctive composition for Apollo 16 impact melts: Ni/Ir averaging ~1.8× chondritic. In contrast, lunaite impact-melt breccias have consistently chondritic Ni/Ir. Impact melts from Luna 20 and other Apollo sites show average Ni/Ir almost as high as those from Apollo 16. The prevalence of this distinctive Ni/Ir ratio at such widely separated nearside sites suggests that debris from one extraordinarily large impact may dominate the megaregolith siderophile component of a nearside region 2300 km or more across.

Highland polymict breccia lunaites and other KREEP-poor highland regolith samples manifest a strong anticorrelation between Al_2O_3 and mg. The magnesian component probably represents the chemical signature of the Mg-suite of pristine nonmare rocks in its most "pure" form, unaltered by the major KREEP-assimilation that is so common among Apollo Mg-suite samples. The average composition of the ferroan anorthositic component is now well constrained at Al_2O_3 ~29–30 wt% (implying about 17–19 wt% modal mafic silicates), in good agreement with the composition predicted for flotation crust over a "ferroan" magma ocean (Warren 1990).

INTRODUCTION

The 19 or more lunar meteorites (lunaites) represent a valuable adjunct to the samples brought from the Moon by artificial means on the Apollo and Luna missions. Lunaite source craters are probably distributed almost randomly across the Moon's surface (Warren and Kallemeyn 1991). In contrast, the six Apollo and the three Luna sites were confined to a small region of the central nearside. A polygon can be contrived to encompass all nine sites and yet still cover only 4.4% of the surface of the Moon. Site-to-site variation among Apollo rocks is generally much greater between missions (the average separation from nearest-neighbor site is 420 km) than between two ends of a single mission's traverse range (separations ≤11 km).

Orbital spectrometry has also furnished data for surface regolith composition (e.g., Metzger et al. 1977; Lawrence et al. 2003) that is global in coverage, but only for a few elements, and with limited sensitivity and precision. Even so, these orbital data indicate a remarkable degree of 1000-km scale heterogeneity, especially in terms of abundance of thorium and other incompatible elements (Lawrence et al. 2003; Elphic et al. 2000). The main focus of this paper and its companion (Warren 2005) is to adduce new data for lunaites and to employ these and earlier data for lunaites and Apollo and Luna samples as a form of ground truth with which to test and, if necessary, improve the current Lawrence et al. (2003) calibration of the Lunar Prospector gamma ray spectrometry data for thorium. The orbital Th data can be applied to estimate the bulk composition of the lunar crust and of the whole Moon as constraints on the Moon's evolution, and especially on its origin.

The number of discrete lunaites is presently ~20–25; the exact tally depends, for example, on whether three recently found lunaites from the Dhofar region of Oman (Nazarov et al. 2002) are paired with one of the three previously known Dhofar lunaites. In this paper, several "new" or nearly new lunaites, including the first three lunaite impact-melt breccias, are described and compared with their Apollo/Luna counterparts in terms of both incompatible and siderophile trace elements. The highland lunaite population as a whole, emphasizing KREEP-poor samples, is scrutinized for clues to the nature of the ferroan-anorthositic and magnesian components of the lunar crust. Particular emphasis is placed on thorium, which, being well-suited to global gamma ray spectrometric analysis (Lawrence et al. 2003) as well as an exemplary refractory-lithophile element, can potentially provide a foundation for constraining the overall composition of the Moon (Warren 2005). Moreover, Th is a tracer for petrologically "evolved" crust.

EXPERIMENTAL METHODS

Sample bulk compositions were determined primarily using instrumental neutron activation analysis (INAA), following the procedure of Kallemeyn (1993). Irradiations for INAA were obtained at the University of California—Irvine reactor facility. INAA typically begins with a 2-minute "rabbit" irradiation, followed by a single 2-minute count to determine short-lived species: Mg, Al, Ti, V, Mn, and Ca. Other elements (and replicate data for Mn and Ca) are determined after a subsequent 4-hour irradiation through a series of 4–5 separate, increasingly long counts that finally end about two months after the irradiation. Data analysis is based on the program SPECTRA (Grossman and Baedecker 1986), which achieves optimal precision through the use of graphic display and interactive analysis of the γ-ray spectra. Integrations of the areas of small γ-ray peaks and multiplets are checked visually and baseline parameters are adjusted where necessary.

In most cases, each chip sample was crushed to fine powder prior to INAA using an agate mortar and pestle. If so, a small aliquot (generally 5–25 mg, depending on the overall sample size) of the powder was set aside for analysis by the microprobe fused-bead analysis (MFBA) technique. In MFBA, the powder is fused on a Mo strip heater under an Ar atmosphere. The glass bead is then mounted and analyzed by straightforward electron probe microanalysis to determine major elements, most notably Si, which we do not determine by INAA. Volatile loss is not a serious concern because Na and K are well determined by INAA. Analysis results are presented in Table 1. It should be noted that, for the purposes of figures and discussion, we generally use averages of all available literature data rather than relying exclusively upon our own data, because the few labs working on lunaites are all of high quality, and when dealing with small samples of lunar breccias, disparate results are more commonly caused by sample heterogeneity than by analytical error.

Backscattered electron images of thin sections were acquired using an LEO 1430 scanning electron microscope. Phase analyses were obtained using wavelength-dispersive detectors on a Cameca Camebax electron probe, running at an accelerating voltage of 15 KV, with typical count durations of 15–20 sec.

SAMPLE DESCRIPTIONS

The following descriptions are weighted toward samples like Dhofar 081 and especially Dhofar 026, which are not easily classified. Note that weathering effects are discussed mainly in a separate section below. Like most other lunaites (Warren 1994, 2001), nearly all these new samples were remarkably hard to crush during preparation for our analyses and were far more cohesive than all of the asteroid-crustal achondrites (e.g., many tens of eucrites) that we have processed over the years. The only clear exception was NWA 482, which crushed easily, but Y-981031 was also easier to crush than most lunaites.

Regolith Breccias

Dar al Gani (DaG) 262

Bischoff et al. (1998) characterized this 513 g highland regolith breccia in considerable detail. Its high concentrations of noble gases suggest thorough blending of the source-regional rock debris. The reported concentration of ^{36}Ar, a noble gas that correlates with other maturity indices among Apollo surface soils (McKay et al. 1991), implies that by the standards of surface soils (Morris 1978), DaG 262 may be classed as submature. Our results (Table 1) show good agreement with previous analyses (Bischoff et al. 1998; Nishiizumi et al. 1998; Korotev et al. 2003a), except for Br, where our result seems especially altered by terrestrial weathering.

Table 1. Concentrations of 40 elements in bulk-rock samples of lunar meteorites.

	Mass (mg)	Na mg/g	Mg mg/g	Al mg/g	Si mg/g	K mg/g	Ca mg/g	Sc μg/g	Ti mg/g	V μg/g	Cr mg/g	Mn mg/g	Fe mg/g	Co μg/g	Ni μg/g	Ga μg/g	As μg/g	Br μg/g	Sr μg/g
Normal uncertainty[a]		3%	4%	4%	3%	7%	4%	3%	5%	5%	4%	3%	4%	3%	5%	8%	12%	10%	10%
Regolith breccias																			
DaG 262A	126	2.59	32.4	148	207	0.56	117	8.4	1.5	10	0.66	0.50	35.1	22.2	230	4.4	<1.0	5.5[c]	176
Notable uncertainties[a]						16			11	25									
DaG 262B	231	2.45	32.1	145	207	0.85	124	8.0	1.1	26	0.62	0.48	33.6	17.9	186	4.3	0.21	3.4[c]	209
Notable uncertainties[a]																12			
Dhofar 025	104	2.53	38.4	141	209	0.45	112	9.8	1.8	23	0.81	0.57	37.5	15.3	113	3.1	0.17	1.11	1410[c]
Notable uncertainties[a]										15									
QUE 93069,8A	267	2.39	27.0	155	209	0.29	118	7.2	1.74	29	0.53	0.54	32.4	22.2	270	3.0	–	–	140
Notable uncertainties[a]																			
QUE 93069,8B	268	2.35	26.4	151	210	0.33	115	7.2	1.56	19	0.56	0.46	32.1	21.2	288	3.1	0.06	<0.1	145
Notable uncertainties[a]																9	33		
QUE 94269,14	261	2.38	26.1	149	209	0.22	119	7.4	1.49	17.0	0.55	0.44	34.1	21.9	286	3.4	<0.10	0.30	147
Notable uncertainties[a]																9			
Y-981031;69	241	3.08	51.0	95.1	217	0.60	89.2	26.4	3.5	72	1.81	1.18	91.5	39.7	159	3.9	<0.26	2.2	95
Notable uncertainties[a]																			11
Fragmental breccia																			
Dhofar 081	408	2.27	16.9	165	209	0.17	126	5.8	0.89	19	0.38	0.37	23.6	10.4	94	2.4	<0.06	0.35	280[c]
Notable uncertainties[a]						9			14	16									
Impact-melt breccias																			
DaG 400	146	2.35	29.0	143	201	0.66	142[c]	6.4	0.84	23	0.50	0.54	28.9	15.1	160	2.9	1.02[c]	3.6[c]	300[c]
Notable uncertainties[a]									13	15						9			
NWA 482	186	2.82	24.9	154	210	0.30	119	7.1	1.10	16	0.51	0.44	30.3	14.5	170	3.3	<0.12	2.1	127
Notable uncertainties[a]										17						10			
Dhofar 026[§]	57	2.50	40	143	209	0.38	116	8.7	1.7	<20	0.63	0.53	36.5	16.2	155	3.7	<0.15	1.7	128
Notable uncertainties[a]						11										9			
Dhofar 457	241	2.42	25.5	150	210	0.32	121	8.3	1.0	16	0.62	0.54	33.9	17.3	153	4.3	<0.26	1.9	209
Notable uncertainties[a]									20	18									
Dhofar 458	274	2.39	24.8	153	210	0.33	120	7.5	1.3	18	0.56	0.52	31.9	16.0	138	3.8	0.18	1.9	254[c]
Notable uncertainties[a]						10			12	25							31		
Dhofar 459	185	2.31	24	155	211	0.31	119	7.9	1.3	15	0.61	0.59	30.8	16.6	125	3.3	0.10	1.6	540[c]
Notable uncertainties[a]										12							22		
Dhofar 461	234	2.28	24	155	210	0.31	119	7.4	1.3	15	0.55	0.47	31.7	14.8	116	3.1	<0.16	1.34	350[c]
Notable uncertainties[a]										14									
Dhofar 462	173	2.33	24.9	153	210	0.28	121	7.6	1.2	20	0.57	0.45	32.8	16.4	147	3.8	<0.36	2.8	206
Notable uncertainties[a]									14	14									
Dhofar 463	300	1.61	24	155	210	0.26	120	7.5	1.0	20	0.57	0.45	30.3	16.0	134	3.9	0.17	1.20	890[c]
Notable uncertainties[a]									15								13		

Table 1. *Continued.* Concentrations of 40 elements in bulk-rock samples of lunar meteorites.

	Mass (mg)	Na mg/g	Mg mg/g	Al mg/g	Si mg/g	K mg/g	Ca mg/g	Sc µg/g	Ti mg/g	V µg/g	Cr mg/g	Mn mg/g	Fe mg/g	Co µg/g	Ni µg/g	Ga µg/g	As µg/g	Br µg/g	Sr µg/g
Dhofar 464	272	2.36	25	154	210	0.29	120	7.8	1.2	18	0.59	0.46	31.3	15.5	127	3.7	<0.20	1.36	630[c]
Notable uncertainties[a]									10	8									
Dhofar 465	259	2.37	24	155	209	0.32	122	7.8	1.2	23	0.59	0.55	31.1	16.0	127	3.5	<0.21	1.8	670[c]
Notable uncertainties[a]										8									
Dhofar 466	481	2.25	21.8	156	209	0.28	124	7.1	1.4	18	0.52	0.43	29.4	13.2	118	2.7	<0.10	1.13	310[c]
Notable uncertainties[a]									15	14									
Dhofar 467	249	2.24	26	151	209	0.31	121	7.7	1.1	22	0.58	0.54	33.9	15.7	136	3.4	<0.34	1.9	300[c]
Notable uncertainties[a]									14	8									
Dhofar 468	227	2.22	25	151	210	0.33	120	7.5	1.4	18	0.55	0.48	31.2	17.0	174	3.3	0.15	2.1	1260[c]
Notable uncertainties[a]									14	15							30		
Dhofar 026-MW mean[§]		2.24	24.5	154	210	0.30	121	7.6	1.2	19	0.57	0.49	31.5	15.6	134	3.5	–	1.6	497[c]

Table 1. Concentrations of 40 elements in bulk-rock samples of lunar meteorites.

	Zr µg/g	Sb ng/g	Cs ng/g	Ba µg/g	La µg/g	Ce µg/g	Nd µg/g	Sm µg/g	Eu µg/g	Tb µg/g	Dy µg/g	Ho µg/g	Yb µg/g	Lu µg/g	Hf µg/g	Ta µg/g	Ir ng/g	Au ng/g	Th µg/g	U µg/g
Normal uncertainty[a]	9%	12%	11%	9%	4%	7%	7%	4%	4%	6%	8%	8%	5%	5%	6%	10%	5%	6%	7%	10%
Regolith breccias																				
DaG 262A	37	<70	<120	240[c]	2.65	6.6	4.2	1.22	0.86	0.25	1.81	0.37	1.00	0.143	0.87	0.130	10.4	7.0[c]	0.38	0.069
Notable uncertainties[a]	26						8													
DaG 262B	<30	41	<120	117[c]	2.25	5.3	3.3	1.01	0.74	0.21	1.5	0.26	0.79	0.110	0.78	0.114	9.8	4.6	0.38	0.160
Notable uncertainties[a]											12									
Dhofar 025	42	22	<20	110[c]	3.0	7.4	4.7	1.35	0.74	0.27	1.6	0.38	1.07	0.160	0.98	0.130	4.5	4.9[c]	0.46	0.19
Notable uncertainties[a]	16	23									35									
QUE 93069,8A	46	23	–	42	3.7	8.8	5.7	1.63	0.79	0.35	–	0.51	1.25	0.179	1.16	0.156	11.2	4.5	0.55	0.138
Notable uncertainties[a]	21	25		20			8													
QUE 93069,8B	38	13	100	42	3.17	7.9	4.7	1.48	0.78	0.31	2.04	0.38	1.12	0.16	1.08	0.148	22	5.1	0.57	0.11
Notable uncertainties[a]	25	39	30	11																
QUE 94269,14	43	<800	<60	35	3.17	7.2	4.0	1.44	0.84	0.29	1.8	0.37	1.14	0.17	1.06	0.130	14.2	4.6	0.44	0.10
Notable uncertainties[a]	20			20			10				11									23
Y-981031;69	80	<100	100	101	7.7	19.1	12.4	3.6	0.99	0.77	5.3	0.99	2.82	0.395	2.93	0.352	4.5	2.3	1.03	0.19
Notable uncertainties[a]	13		24														7	16		
Fragmental breccia																				
Dhofar 081	<20	<7	38	20	1.43	3.6	1.96	0.60	0.85	0.139	<0.89	0.18	0.53	0.074	0.49	0.067	4.8	5.5[c]	0.20	0.075
Notable uncertainties[a]			12	14																
Impact-melt breccias																				
DaG 400	<24	72[c]	66	820[c]	2.50[c]	5.3[c]	2.6	0.93	0.78	0.21	1.36	0.25	0.73	0.078	0.65	0.107	5.3	2.3	0.37	0.58[c]
Notable uncertainties[a]							11				11							7		
NWA 482	<29	<6	<52	30	1.55	3.5	2.45	0.77	0.79	0.172	1.3	0.21	0.67	0.097	0.60	0.092	5.9	2.8	0.23	0.052
Notable uncertainties[a]											11									17

Table 1. *Continued.* Concentrations of 40 elements in bulk-rock samples of lunar meteorites.

	Zr µg/g	Sb ng/g	Cs ng/g	Ba µg/g	La µg/g	Ce µg/g	Nd µg/g	Sm µg/g	Eu µg/g	Tb µg/g	Dy µg/g	Ho µg/g	Yb µg/g	Lu µg/g	Hf µg/g	Ta µg/g	Ir ng/g	Au ng/g	Th µg/g	U µg/g
Dhofar 026§	56	42[c]	<50	52	3.1	7.3	5.0	1.39	0.78	0.27	<1.34	0.35	1.01	0.150	0.99	0.10	487[c]	4.1	0.47	0.15
Notable uncertainties[a]	19	16		12			8									15		8		
Dhofar 457	34	<150	126[c]	81	3.8	7.9	5.3	1.45	0.86	0.28	1.94	0.43	1.13	0.152	1.01	0.140	13.0	7.8	0.45	0.15
Notable uncertainties[a]	22											11								
Dhofar 458	46	48[c]	71	168[c]	3.06	6.8	4.0	1.22	0.79	0.26	1.76	0.37	0.94	0.134	0.83	0.116	5.2	11.4[c]	0.37	0.13
Notable uncertainties[a]	19	30	22									9								
Dhofar 459	16	40	85[c]	430[c]	2.48	6.3	3.2	1.09	0.78	0.26	1.53	0.29	0.89	0.131	0.80	0.109	5.6	17.8[c]	0.37	0.181
Notable uncertainties[a]	29	12	17																	
Dhofar 461	<50	21	82	109[c]	2.30	5.8	3.6	1.06	0.71	0.25	1.8	0.29	0.88	0.126	0.80	0.101	5.3	16.1[c]	0.34	0.127
Notable uncertainties[a]		28	16									11								9
Dhofar 462	39	34	81	79[c]	2.66	6.2	3.6	1.16	0.79	0.23	1.54	0.35	0.93	0.130	0.87	0.125	6.3	23.7[c]	0.38	0.075
Notable uncertainties[a]	17	27	18				8													10
Dhofar 463	33	24	82	350[c]	2.5	6.1	3.6	1.05	0.69	0.25	1.08	0.26	0.83	0.123	0.79	0.106	6.1	10.4[c]	0.34	0.23
Notable uncertainties[a]	14	16	12																	
Dhofar 464	33	<170	74	121[c]	2.92	6.4	4.1	1.24	0.76	0.27	1.59	0.41	0.95	0.135	0.84	0.107	5.5	19.8[c]	0.39	<0.13
Notable uncertainties[a]	17		14								9	12						9		
Dhofar 465	33	<40	85	320[c]	2.95	6.1	4.1	1.15	0.78	0.25	1.41	0.31	0.87	0.124	0.77	0.095	5.2	17.6[c]	0.35	<0.11
Notable uncertainties[a]	17		16									15						10		
Dhofar 466	30	36	58	220[c]	2.30	4.9	3.0	0.94	0.75	0.20	1.4	0.30	0.78	0.104	0.66	0.102	4.6	6.3[c]	0.27	0.078
Notable uncertainties[a]	17	36	14								11									10
Dhofar 467	36	<40	69	165[c]	3.08	6.3	4.1	1.22	0.73	0.27	1.8	0.32	0.92	0.136	0.90	0.116	6.5	5.3[c]	0.40	<0.13
Notable uncertainties[a]	17		17									13						33		
Dhofar 468	49	66[c]	<120	1340[c]	2.57	5.8	3.8	1.08	0.73	0.23	1.53	0.28	0.88	0.126	0.81	0.116	7.1	13.4[c]	0.33	0.092
Notable uncertainties[a]	16	17					25													
Dhofar 026-MW mean[b]	35	38	78[c]	391[c]	2.76	6.2	3.8	1.14	0.76	0.25	1.55	0.33	0.90	0.127	0.81	0.111	15.5	12.5[c]	0.36	0.13

[a]Uncertainties are shown where they are larger than normal 70% confidence levels (i.e., "normal" for moderate-high concentrations).

[b]Mass-weighted (MW) mean of the 12 Dhofar 026/468 analyses; for the sample of the original Dhofar 026 stone, we also found 930 (±18%) ng/g of Ru, 44 (±8%) ng/g of Re and 520 (±9%) ng/g of Os.

[c]Suspiciously high concentrations that seem likely to reflect terrestrial weathering are highlighted.

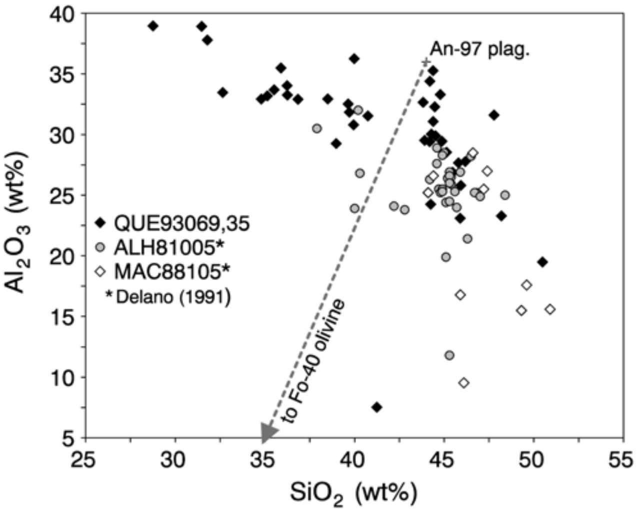

Fig. 1. On a plot of SiO_2 versus Al_2O_3, a large proportion of QUE 93069 glass spherules show HASP affinity, as they plot well to the low-Si side of a join between extraordinarily anorthitic plagioclase and extraordinarily ferroan olivine. Also shown for comparison are data for glass spherules from two other highland lunaite regolith breccias (Delano 1991).

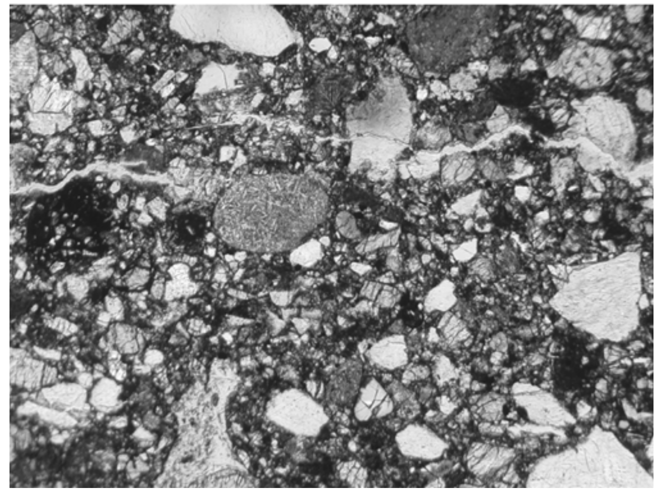

Fig. 2. Transmitted light photomicrograph of regolith breccia Y-981031. The area shown is typical of the breccia matrix, except for the presence (near center) of a spheroidal clast of extremely fine-grained, but crystalline, impact-melt breccia. Width of view: 3.1 mm.

Dhofar 025

This 750 g highland regolith breccia (Taylor et al. 2001) is relatively immature as a regolith sample, based on its noble gas contents (Shukolyukov et al. 2001). Our bulk-rock results show generally good agreement with two previous analyses (Taylor et al. 2001; Korotev et al. 2003a), but we do not confirm the high Eu (1.3 μg/g) reported by Taylor et al. (2001), and trace elements, both incompatible and siderophile, are relatively low in our sample. Our Sr result is much lower, but still shows major desert evaporite contamination. Our data, and the Korotev et al. (2003a) results especially, show abnormally high Au/Ir and Au/Ni, but higher Au might merely represent contamination during handling.

Queen Alexandra Range (QUE) 93069 and 94269

These are paired samples (21 and 3 g, respectively) of a single mature highland regolith breccia. Its concentrations of noble gases (e.g., Shukolyukov et al. 2001) are high, even by the standards of surface soils. As a mature regolith sample, it is rich in regolith (mostly impact-splash-melt) glass spherules, of which a remarkably large proportion show high-alumina, silica-poor (HASP) compositions, akin to the materials first given this name by Naney et al. (1976). On a plot of SiO_2 versus Al_2O_3 (Fig. 1), 18 of 39 of nonmare glass spherules and spherule fragments analyzed (at least 2 and mostly 3–4 analyses averaged for each glass) plot to the low-SiO_2 side of a join between anorthitic plagioclase and an extremely SiO_2-poor variety (Fo_{40} olivine) of nonmare mafic silicate. The proportion of HASP compositions is even higher among glasses of relatively small (estimated spheroidal) diameter d_{es}. For example, 11 out of 14 of the nonmare glasses with $d_{es} < 50$ μm plot to the left of the An_{97}-Fo_{40} join in Fig. 1. Such a relationship could be a consequence of surface area/volume ratio having influenced volatilization. However, Kempa and Papike (1980) found no relationship between spheroid size and HASP composition among Apollo 16 soil samples. Our bulk compositional data show good agreement with previous data for QUE 93069 (Lindstrom et al. 1995; Spettel et al. 1995; Koeberl et al. 1996; Korotev et al. 1996; Nishiizumi et al. 1996; Thalmann et al. 1996), and, as expected, strong similarity between QUE 93069 and 94269. Like most lunar regolith samples of high maturity (cf. Warren 2004), QUE 93069/4269 is uncommonly rich in highly siderophile elements (Ni, Ir, and Au).

Yamato- (Y-) 981031

This 186 g regolith breccia is paired with Y-793274 (Arai et al. 2002; Lorenzetti and Eugster 2002; Korotev et al. 2003a), and as discussed by Arai and Warren (1999; cf. Jolliff et al. 1998), Y-793274 is probably launch-paired with QUE 94281, albeit these “YQ” stones were found on opposite sides of Antarctica. Like QUE 94281 (Arai and Warren 1999), Y-981031 contains a smattering of round impact-melt breccia clasts, of the type called “crystalline lunar spherules” (CLS) by Symes et al. (1998) (Fig. 2; cf. Dhofar 026, described below). Meteorite Hills (MET) 01210 is probably launch-paired with the YQ stones Y-793274/981031 and QUE 94281 (e.g., Arai et al. 2005).

Our data show generally good agreement with previous analyses of relatively feldspar- (Al_2O_3) rich pieces of Y-793274 and QUE 94281 (Arai and Warren 1999 and references therein), including the two previous analyses of Y-981031 (Kojima 2000; Korotev et al. 2003b). All of these YQ samples are, to a good approximation, binary mixtures of

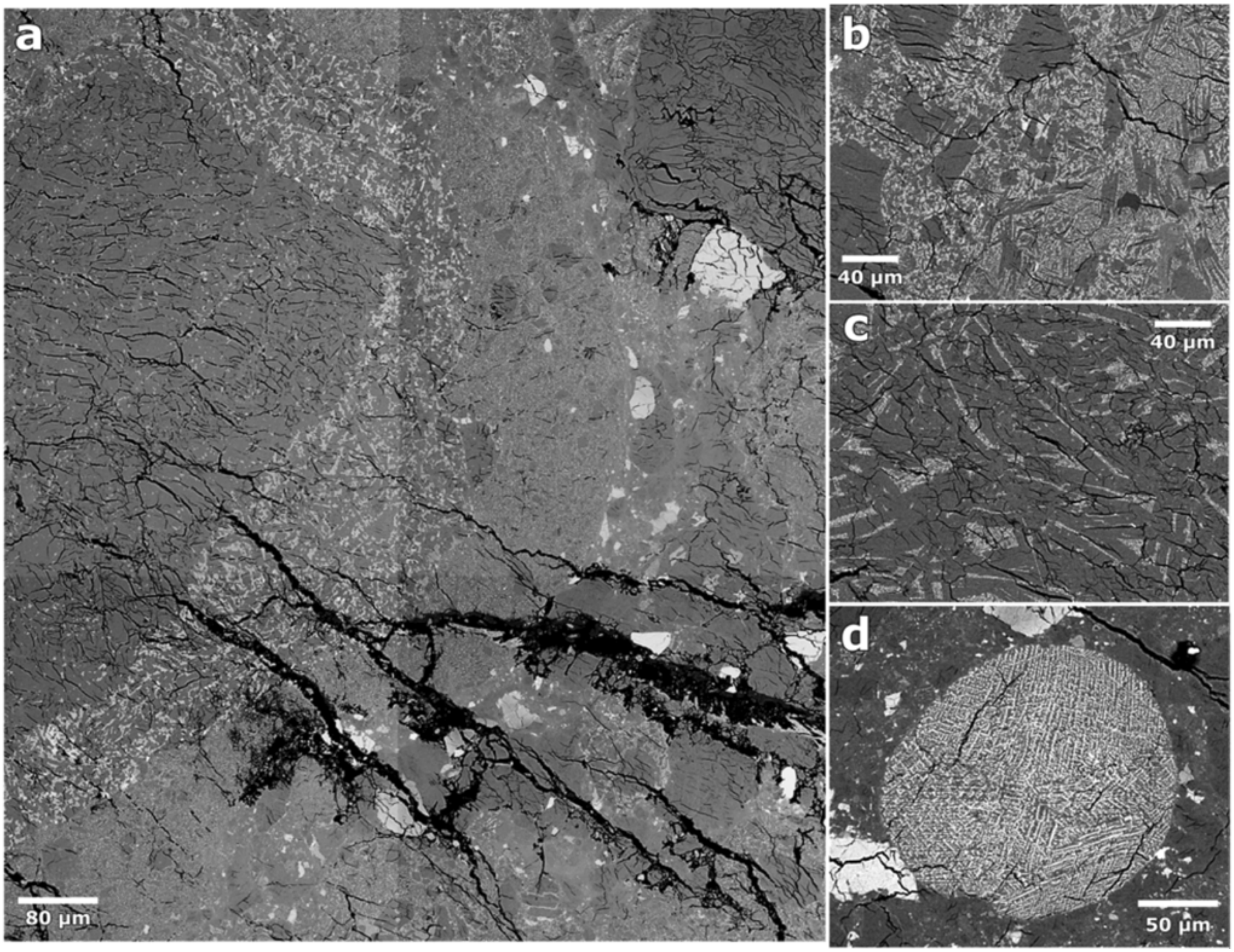

Fig. 3. Backscattered electron images of regolith(?) breccia DaG 400, giving some indication of the variety of impact melt clast types within this complex breccia. a) The large anorthositic clast at left was completely sheathed by a mafic variety of impact melt before the final (anorthositic) impact-melt breccia formed. b) Another unusually mafic impact-melt breccia; the variolitic texture (along right edge) is typical of this clast. c) A more anorthositic variety of impact-melt breccia. d) A vitrophyric spherule that is probably an impact melt; rastered-beam analysis indicates a nonmare composition (16 wt% Al_2O_3, 0.3 wt% TiO_2, mg ~62 mol%). The only other unambiguously spheroidal object found in this 100 mm^2 sample of DaG 400 is anorthositic (28 wt% Al_2O_3).

subequal proportions of nonmare regolithic debris and a mare basalt component, and our new data conform to the mare-highland mixing trends previously observed (Jolliff et al. 1998; Arai and Warren 1999). The YQ mare component is dominantly VLT, and the YQ highland component has moderate incompatible element concentrations, e.g., Th ~1.4 µg/g (Arai and Warren 1999).

Three Difficult-to-Classify Highland Breccias: DaG 400, Dhofar 026, and Dhofar 081

Regolith(?) Breccia Dar al Gani (DaG) 400

At 1425 g, DaG 400 is the largest lunaite yet found. Zipfel et al. (1998), Cohen et al. (1999), and Korotev et al. (2003a) have very briefly described DaG 400 as a highland regolith breccia rich in impact-melt breccia clasts. However, the noble gas contents in DaG 400 are low (Scherer et al. 1998; Shukolyukov et al. 2001), and the "three small thin sections" studied by Bukovanska et al. (1999) consist of impact-melt breccia. The 100 mm^2 thin section we have studied is dominantly a clast-rich, crystalline impact-melt breccia (Fig. 3). Most of the clasts are themselves impact-melt breccias with a wide variety of modal plagioclase/mafic silicate ratio. A handful (3–5) of apparent regolith glassy spherules can be seen in the matrix, although only two of these are unambiguously quenched glassy spherules (Fig. 3d). The Y-82192/6032 lunaite is a precedent for a breccia that contains numerous unambiguous regolith spherules (Bischoff et al. 1987; Yanai and Kojima 1987), and yet is widely considered not a regolith breccia but a fragmental breccia (Koeberl et al. 1990; Takeda et al. 1990). However, we assume that DaG 400 as a whole is an unusual (extremely immature? reheated?) variety of regolith breccia.

For most elements, our bulk-rock compositional data

(Table 1) agree fairly well with previous analyses (Zipfel et al. 1998; Bukovanska et al. 1999; Korotev et al. 2003a). However, elements such as Ba, Sr, and U, and also high ratios of light REE to Lu, indicate especially severe weathering effects in our sample. The oddly high Ca in our analysis is probably also a weathering ($CaCO_3$) effect; Korotev et al. (2003a) also suspected calcite as the cause of high Ca in one of their two subsamples. Both our analysis and that of Korotev et al. (2003a) imply an enigmatically low Fe/Mn ratio (53-52). However, Zipfel et al. (1998) found a lower Mn (0.40 mg/g) along with slightly higher Fe, and thus normal lunar Fe/Mn (73). Possibly the high-Mn samples reflect an Mn-carbonate component and/or less olivine. According to Bukovanska et al. (1999), Fe/Mn is constant at ~100 in DaG 400 olivine, but far lower in the pyroxene.

Impact-Melt(?) Breccia Dhofar 026

This anorthositic sample has a unique texture that is difficult to classify. Cohen et al. (2001) classified it as an impact-melt breccia, but Cohen et al. (2004), who describe its petrography in great detail, reinterpreted it as an impact-heated granulitic breccia. As discussed in a later section, we prefer to consider Dhofar 026 an unusual variety of impact-melt breccia. The most distinctive aspect of its texture is a modally very minor (<<1%) component: ovoid globules that are consistently fine-grained and incongruously (in this highly anorthositic breccia) subophitic-mafic (Fig. 4). Roughly half of the breccia consists of an aphanitic component that, over length-scales of order 0.1 mm, is nearly monomineralic plagioclase, and appears to be recrystallized maskelynite (however, our samples include a few scattered mm-sized grains that retain "aggregate" extinction). The other approximately one-half of the breccia has a partially poikilitic "intergrowth" texture that is in many respects intermediate between the near-monomineralic plagioclase component and the globules. Boundaries between Dhofar 026 textural domains tend to be gradational, but Cohen et al. (2004) further subdivide the intergrowth component into pyroxene-plagioclase intergrowths, olivine-plagioclase intergrowths, and a minor component of isolated "relict" olivines.

For this study, in addition to analyzing a small chip from the original Dhofar 026 (a 148 g stone), we received samples from 11 out of a set of 12 different stones (original masses from 19 to 100 g, average 49 g) all acquired by the Labennes from a limited (1.8 km across) area close to the original find site of Dhofar 026. A quick inspection of thin sections with the SEM was sufficient to verify that all these 11 samples are pieces of the same original rock as Dhofar 026, because all feature the same distinctive texture of a highly feldspathic aphanitic-poikilitic matrix with intergrowth areas that may include partially digested (or partially coalesced?) globules; in nearly all cases one or more of the distinctively ovoid intact globules are also found (Fig. 4). Also, J.-A. Barrat has kindly shared with us an unpublished analysis (by ICP-MS) of the Labennes' twelfth stone from the Dhofar 026 area; his analysis, apart from relatively milder weathering effects, is practically identical to our average for Dhofar 026 (Table 1). These 12 "new" Dhofar 026 stones have been assigned provisional names of Dhofars 457–468; the Barrat sample is Dhofar 462.

Our bulk-rock data also agree fairly well with the analysis by Taylor et al. (2001) of the original Dhofar 026 stone. One difference is generally higher Na (average 2.24 mg/g) than found by Taylor et al. (1.80 mg/g). Our small chip of the original Dhofar 026 stone contained remarkably high, approximately chondritic concentrations of highly siderophile elements Ru, Re, Os, and Ir, even though these elements are at normal levels (roughly 0.02× CI-chondritic for a lunar polymict breccia) in all other Dhofar 026 analyses, and Ni and Au are not significantly higher in the Ir-rich sample than in average Dhofar 026. For Ir and Os, the anomalously high results are from two separate counts (and in the case of Ir also two separate peaks), so the anomaly can hardly be an artifact of faulty INAA. Ordinary handling contamination seems unlikely because the easiest element to contaminate by ordinary handling is Au. But this sample was only 57 mg and sawn on all sides. Conceivably, it may have acquired a small proportion of cross-contamination from a sample of a CAI-bearing chondrite, or it may contain CAI components as a result of admixture during the natural process of impact melting. Allende CAIs contain "platinum-group alloy nuggets" with Ru, Re, Os, and Ir at concentrations of order 1000× CI and yet relatively low Ni and Au (e.g., Ni of order 1× CI) (Wark 1987). However, even the largest of 20 such nuggets studied by Wark (1987) would individually be about 10^5 times too low in mass to account for the enigmatic Dhofar 026 data. We can only speculate that the sample (now an irradiated powder) may contain a very extraordinarily large nugget of this general type.

Although all of the Labennes' 12 Dhofar lunaites are clearly paired with the original Dhofar 026, there are noteworthy textural variations among these stones and within individual stones. Many of the lithic clasts that retain sharp boundaries are far less mafic than the distinctive globules. A few, most notably a tabular clast in stone 463 (Fig. 4d), have globule-like mineralogy and yet are far from ovoid in shape. Four of the 12 stones consist largely of fluidized veins of a late generation of localized shock-melt: Dhofars 457, 466, and especially 462 and 468. Stone 468 includes a 6 × 3 mm area that consists dominantly of shock-melt (Fig. 4e); several fluidized bands, each about 1 mm wide, extend out from this area. No intact globule was found in the unmelted half of our thin section of stone 468. However, except within ~0.1 mm of the shock veins, textures in the vein-rich stones are similar to textures in stones in which no veins occur (cf. the left side of Fig. 4e and the central portion of Fig. 4a). Thus, we doubt these shock veins represent the heat source invoked by Cohen

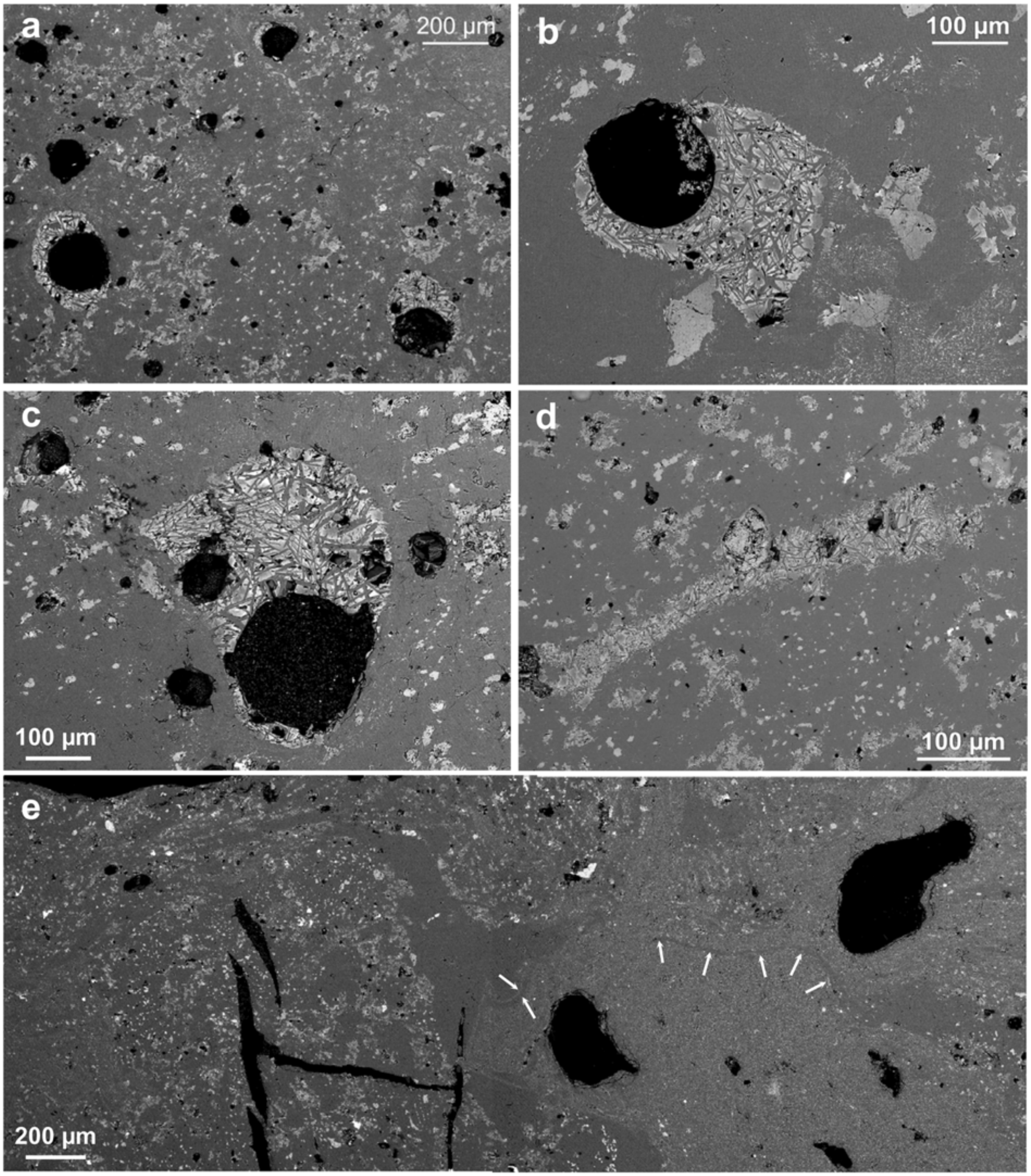

Fig. 4. Backscattered electron images of impact-melt breccia Dhofar 026. a) stone 461: two relatively vesicular but otherwise typical spheroidal mafic impact melt clasts (globules) surrounded by diffuse intergrowth mafic patches. b) A mafic impact melt globule in stone 465 showing one of the most ideally round vesicles in this clast type. Also noteworthy is the odd shape of this clast, mostly spheroidal, but irregular toward the lower right. Further in the same general direction are phenocryst-like coarse pyroxenes and an intergrowth textured patch, features that might reflect partial digestion of this or another nearby mafic clast into the main, final Dhofar 026 impact melt. c) Another example of a mafic impact melt globule (stone 461) consisting largely of an almost perfectly round vesicle. d) Of countless mafic impact melt clasts (and apparent shreds of clasts) in Dhofar 026, this one in stone 463 has the most grossly nonspheroidal shape. Typical effects of terrestrial weathering are evident near the left and top-central margins of the clast and as bright Sr-sulfate grains scattered in the matrix. e) Most of the right half of this view of stone 468 consists of glassy-aphanitic (near-uniform light grey; individual mafic grains are too small to be resolved) shock-melt vein of the type found in several of the stones. The complete glassy, arcuate-anastamosing vein system is too large (centimeter scale) to show here, but narrow glassy bands (arrows) attest to arcuate flow. Note, too, the deformed shapes of vesicles within the vein. The fractures in the otherwise nondescript left-central region appear oddly dilated.

Table 2. Oxide compositions of some components in impact-melt breccia lunaites.

	Dhofar 026				cf. average	NWA 482	
	Bulk	Shock veins	Average bulk globule		Apollo 15	Glass	Bulk
	(Table 1)	(DBA[a])	(DBA[a])	(SEM[a])	IM breccia[b]	vein	(Table 1)
SiO_2, wt%	44.8	44	48	49	47.8	44.9	45.0
TiO_2	0.28	0.5	1.7	1.4	1.4	0.14	0.18
Al_2O_3	29.0	31	13.1	14.7	17.2	29.4	29.1
FeO (t)[c]	4.06	3.8	14.0	14.1	9.2	3.5	3.9
MnO	0.064	–	0.2	–	0.12	0.07	0.057
MgO	4.07	3.0	9.2	8.9	12.2	3.6	4.1
CaO	16.9	18	12.0	10.9	10.8	17.7	16.6
Na_2O	0.30	0.3	0.3	0.5	0.62	0.39	0.38
K_2O	0.037	0.04	0.05	–	0.39	0.03	0.037
Cr_2O_3	0.083	–	0.3	–	0.22	0.07	0.075
Sum	99.6	99.8	99.2	99.5	99.9	99.8	99.5
mg, mol%	0.66	0.58	0.54	0.53	0.70	0.65	0.65
N[d]	12	10	14	3	4 (groups)	10	1

[a]All SEM rastered-area and e-probe DBA results have been corrected for phase-density disparities as recommended by Warren (1997). Correction factors are functions of individual sample mineralogy (i.e., essentially based on the ratio of low-density plagioclase versus high-density mafic phases). The most noteworthy of these correction factors for major elements are in the shock vein DBA: 0.97 for Al_2O_3, 1.22 for FeO, and 1.28 for MgO; in the globule DBA: 0.86 for Al_2O_3, 1.13 for FeO, and 1.08 for MgO; and in the globule SEM analysis: 0.87 for Al_2O_3, 1.14 for FeO, and 1.09 for MgO. However, in the case of the shock-vein DBA, where the target material is glassy (or so fine-grained that X-rays emanate largely from phases beneath the surface), the final results shown above are a compromise: 1:1 averages of raw data and data corrected for the unequal host-phase density effect.

[b]Average of Apollo 15 impact-melt breccia groups A, B, C, and D from Lindstrom et al. (1990).

[c]FeO (t) = total concentration of Fe as FeO.

[d] N = number of analyses averaged.

Compositions for Dhofar 026 include averages from two similarly imprecise techniques: DBA (defocused-beam, 30-µm diameter) e-probe analysis and SEM "semiquantitative analysis" applied to rastered areas of thin sections using a LEO-1430 instrument. The NWA 482 glass vein composition is an average of regular (focused beam) e-probe analyses.

et al. (2004) to cause localized melting by diffusive heating.

The globules are far more mafic than the bulk rock. A typical globule mode has ~45% plagioclase, 35% pyroxene, and 20% olivine. An average of semiquantitative DBA and SEM bulk analyses (Table 2) indicates that the globules resemble the most mafic of the common Apollo impact-melt breccias. Unfortunately, our DBA and SEM bulk analyses cannot measure trace elements. However, our regular bulk-Dhofar 026 data (Table 1) show correlations between Fe and incompatible elements (Fig. 5), paralleling the general trend for incompatible elements to be higher in mafic lunar highland materials than in anorthositic ones (Fig. 6).

Bulk globule analyses (Table 2; also Table 5 of Cohen et al. 2004) are consistently, distinctly ferroan in comparison to the mafic component of the breccia as a whole. Mineral-composition data confirm this relationship. In groundmass areas with the "pyroxene-plagioclase intergrowth" texture of Cohen et al. (2004), olivine tends to be consistently magnesian, Fo_{84-74}, average $Fo_{79.5}$ ± (1σ, 36 analyses) 2.4. In the globules, olivines are more zoned, Fo_{83-52}, and average $Fo_{73.0}$ ± (1σ, 50 analyses) 7.4. Data in Cohen et al. (2004, Figs. 3 and 4) show the globules also have more ferroan pyroxene and more sodic plagioclase than other components of Dhofar 026.

Cohen et al. (2004) noted that the minerals within the globules show no shock effects and thus inferred that the globules must have crystallized late, after the event that maskelynitized virtually all the rock's plagioclase. However, using standard thin sections, the plagioclase-composition grains within the globules are too thin (generally <10 µm; the mafic grains are not much bigger) to definitively test for undulose/patchy extinction.

Voids, at least some of which are clearly vesicles, are scattered throughout Dhofar 026 and amount to roughly 1 vol% of the rock. Most voids are smaller than 100 µm across. However, two ovoid vesicles in shock-melt zones of stone 468 are much larger at ~1000 × 400 µm. The globules are far more vesicular than the rock as a whole (Fig. 4).

Fragmental(?) Breccia Dhofar 081

This 174 g highland breccia has been little-studied until now. Greshake et al. (2001) classified it as a "shocked feldspathic fragmental breccia." We concur, but this lithology is difficult to pigeonhole. As documented by Greshake et al. (2001), its abundant clasts are diverse in size, mineralogy, and texture, but more than half of the volume is a highly feldspathic, fine-grained to glassy matrix. In most areas, the matrix is glassy with a fluidized texture (vesicular, generally deep brown, "swirly" schlieren) that clearly formed by localized shock melting (Fig. 7). Thus, the rock might arguably be classified as an impact-melt breccia.

Because the shock melting was so localized to the fine-grained matrix, we will not quarrel with the choice of Greshake et al. (2001) to classify Dhofar 081 as a fragmental breccia. However, the shock melting has obscured the original nature of the matrix. It is possible that this rock was originally an immature regolith breccia. Greshake et al. (2001) noted that "typical regolith components (i.e., glass spherules or agglutinates)" are nowhere to be found. However, spherules can be rare in immature regolith, and would be hard to recognize in such a vesicular, shock-glass-rich matrix. Among lunar breccias, swirly brown glass (as is common in Dhofar 081) is often inferred to be a shock-modified form of soil agglutinates (e.g., Warren et al. 1983). This inference is based on textural resemblance, but also on data such as those of Drozd et al. (1976), who found among Apollo 15 breccias a tight correlation between "brown, swirly" glass (also termed agglutinitic glass) and trapped noble gases (regolith components, par excellence). Data from McKay et al. (1986, 1989) extend this type of correlation to Apollo 16 breccias, albeit McKay et al. (1989) found that in highly shock-compacted regolith breccias (which would include most lunaite regolith breccias) "agglutinates tend to collapse, melt, and otherwise blend into the matrix so that they become difficult to identify." Despite the pervasive shock melting of the Dhofar 081 matrix (Greshake et al. 2001), its noble gas contents (Greshake et al. 2001; Shukolyukov et al. 2001) are marginally higher than in the immature lunaite regolith breccias Dhofar 025 and MAC 88105, and much higher than in nominally fragmental breccia Y-86032, which contains regolith spherules. In summary, Dhofar 081 appears to be a thoroughly polymict fragmental breccia with unusual traits: it is locally shock-melted and likely contains a significant regolith component.

We report in Table 1 the first bulk-rock compositional data for Dhofar 081, apart from an imprecise ("SemiQuant XRF") analysis for 12 elements by Greshake et al. (2001). The MgO concentration, albeit in our analysis not quite as low as that of Greshake et al. (2001), is the lowest among all lunaites; the mg (≡ Mg/[Mg + Fe]) ratio is also unprecedentedly low. Like most highland lunaites, Dhofar 081 has extremely low incompatible element concentrations in comparison to typical highland rocks from the Apollo and Luna sampling of the central nearside.

Crystalline Impact-Melt Breccia: Northwest Africa (NWA) 482

NWA 482, the first lunaite that is unambiguously an impact-melt breccia (Warren and Kallemeyn 2001; Daubar et al. 2002), was found as a single stone of 1015 g. It has a uniform texture of aphanitic impact-melt breccia (Fig. 8), except for isolated large (up to 3 mm) relict plagioclases and anorthositic clasts, and a small proportion of glassy shock melt pockets and veins that crisscross the stone. A 0.1-mm-wide vein of this type cuts across our NWA 482 thin sections (Fig. 8). This shock glass is highly uniform in composition and approximates the bulk meteorite composition (Table 2).

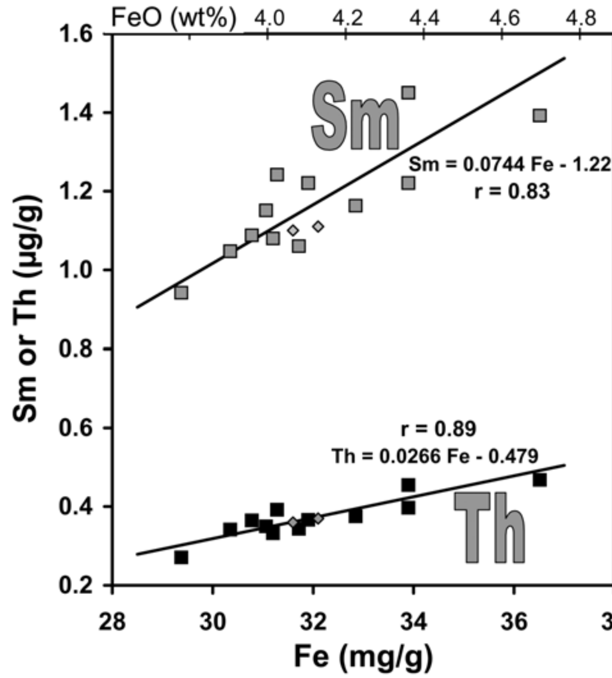

Fig. 5. Fe versus Sm and especially Fe versus Th show significant correlations among bulk analyses of Dhofar 026. Data are mostly from Table 1, but are also (smaller diamond symbols) from Taylor et al. (2001) and J.-A. Barrat (personal communication). When extrapolated, these trends help to constrain the average composition of the Dhofar 026 mafic component, including the subophitic globules.

The groundmass consists of 80–90 vol% plagioclase, subequal amounts of olivine and pigeonitic to subcalcic pyroxene, traces of FeS and carbonate from very mild terrestrial weathering, and little else. Daubar et al. (2002) found a trace of spinel. KREEP-associated phases (K-feldspar, phosphates) have not been found, although there surely must be traces present. Shock melt schlieren and veins seem to be significantly more abundant in lunaites than among the more gently transported Apollo lunar rocks. The NWA 482 glassy-vesicular melt veins and melt pockets loosely resemble the smaller shock melt structures in Dhofar 081 and the wide bands of largely shock melted material in some stones of Dhofar 026 (see above). A long, narrow shock melt vein is also present in QUE 93069 (Warren 2001). Presumably some of these schlieren and veins formed as a result of the violent process of launch off the Moon.

The porosity of NWA 482 is high for a lunaite (roughly 13%, based on thin section observations plus a density measurement of ~2.54 g/cm^3 from the volume of a 21-g slab). Lower porosities prevail among the regolith breccia lunaites, possibly because ordinary porous regolith breccia is too flimsy to survive Moon-Earth transit (Warren 2001).

Our bulk-rock data (Table 1) generally agree well with the results of Korotev et al. (2003a). Our mineral-composition data are shown in Fig. 9. Plagioclase averages $An_{96.3}$ ± 0.7

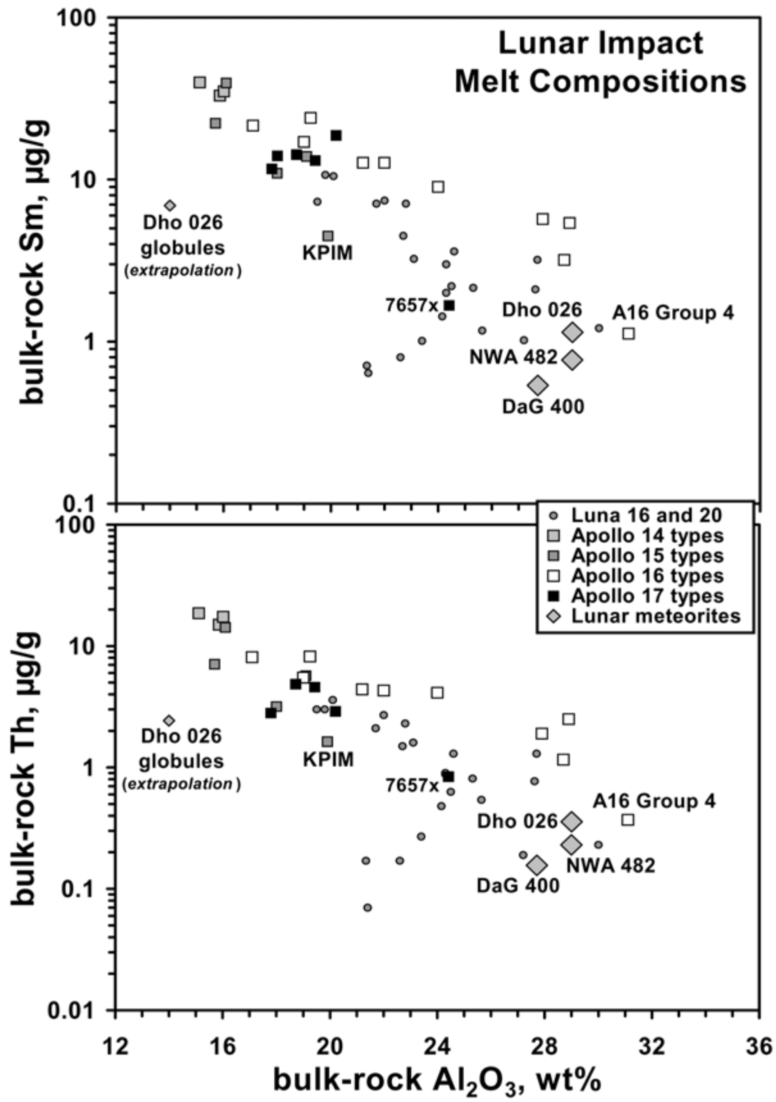

Fig. 6. Al_2O_3 versus (a) Sm and (b) Th in lunar impact-melt breccias. Data for Apollo impact-melt breccias from Korotev (1994), Lindstrom et al. (1990), Meyer (1994), Ryder (1993), Morris et al. (1986), Wänke et al. (1972), and Warren and Wasson (1980). The "7657x" composition is shown with a small symbol because it represents a very poorly sampled group, to our knowledge not previously recognized as a distinct rock type. Data for 7657x are from Meyer (1994) and Warren and Wasson (1978). Note that DaG 400 and Dhofar 026, included here as impact-melt breccias, are difficult to classify; DaG 400 is probably best classified as a regolith breccia dominated by impact-melt components (see text).

(1σ, 24 analyses), with a range of 94.7–98.1. Olivine, where large enough to analyze, averages $Fo_{65.5}$ ± 0.6 (1σ, 23 analyses), range 64.2–66.7, with FeO/MnO = 93 ± 8. Of the relatively few pyroxenes that are large enough to analyze, most fall in a narrow compositional range, with Wo ranging from 11 to 30 mol%, yet with mg uniform at 70 mol%. One exceptional grain yielded several analyses of far more ferroan composition clustered about $En_{42}Wo_{19}$. Daubar et al. (2002) found a wider range, up to $Fo_{77.5}$, for olivine, but a narrower range for pyroxene. In our pyroxene analyses, FeO/MnO averages 52 ± 6, which is typical for lunar pyroxene (Bersch et al. 1991). The pyroxene compositional range is clearly distinct from that found in DaG 400, where very low-Ca ($Wo_{2.4–2.5}$) compositions are common and the range extends to $En_{37}Wo_{41}$ (Bukovanska et al. 1999). The FeNi metals have not been analyzed quantitatively, but energy-dispersive spectra show that most are Ni-rich kamacites, as is typical among polymict lunar impact breccias.

LUNAR PROVENANCE

In most cases, these samples might be presumed lunar on grounds of anorthositic bulk composition alone; thus far, no other parent body has yielded anorthositic meteorites. Detailed study shows that even Y-793274/981031 contains anorthositic clasts (Arai and Warren 1999). Oxygen isotopes

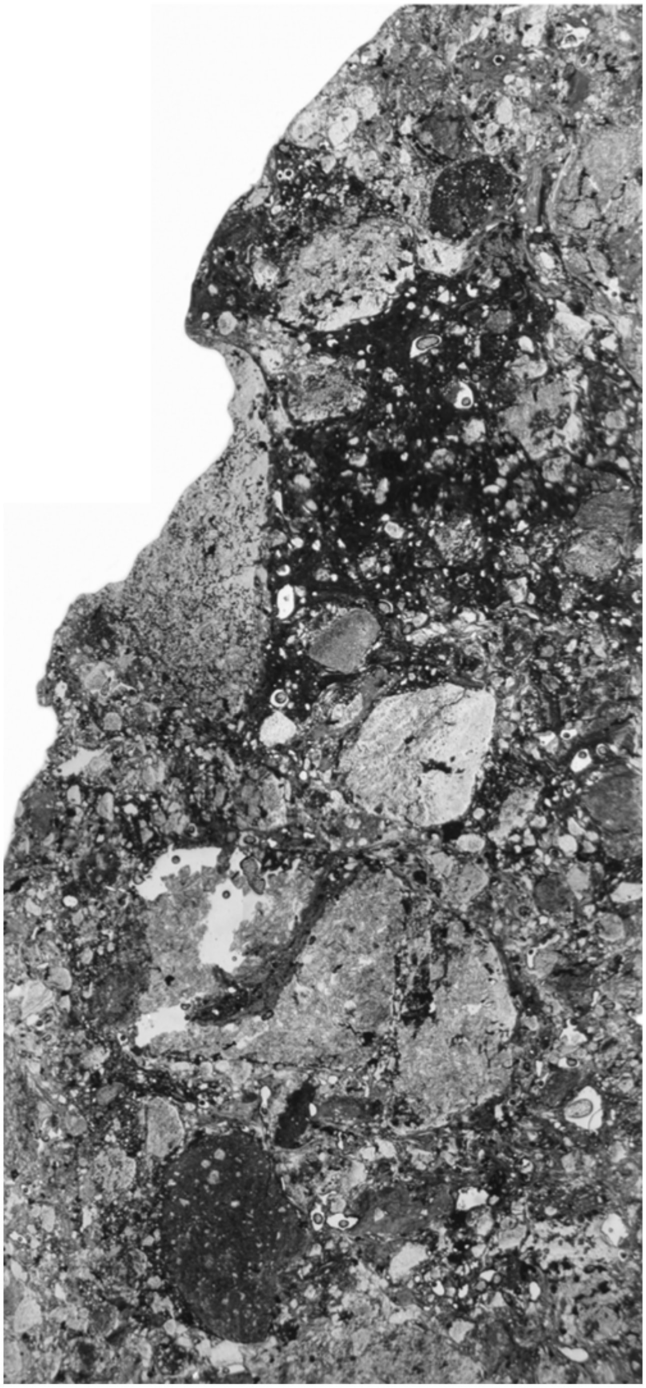

Fig. 7. Transmitted light photomicrograph of fragmental breccia Dhofar 081, showing polymict texture with swirly brown glass (upper right, center, and lower right).

are perhaps the most rigorous test for lunar provenance. Lunar O-isotopic compositions have been determined for most of the samples in this study, e.g., for DaG 262 by Bischoff et al. (1998) for Dhofar 025 and 026 by Taylor et al. (2001). Also helpful for distinguishing lunar from other types of meteorites are ratios of elements that remain cohesive within the lunar crust after tending to be fractionated by solar system

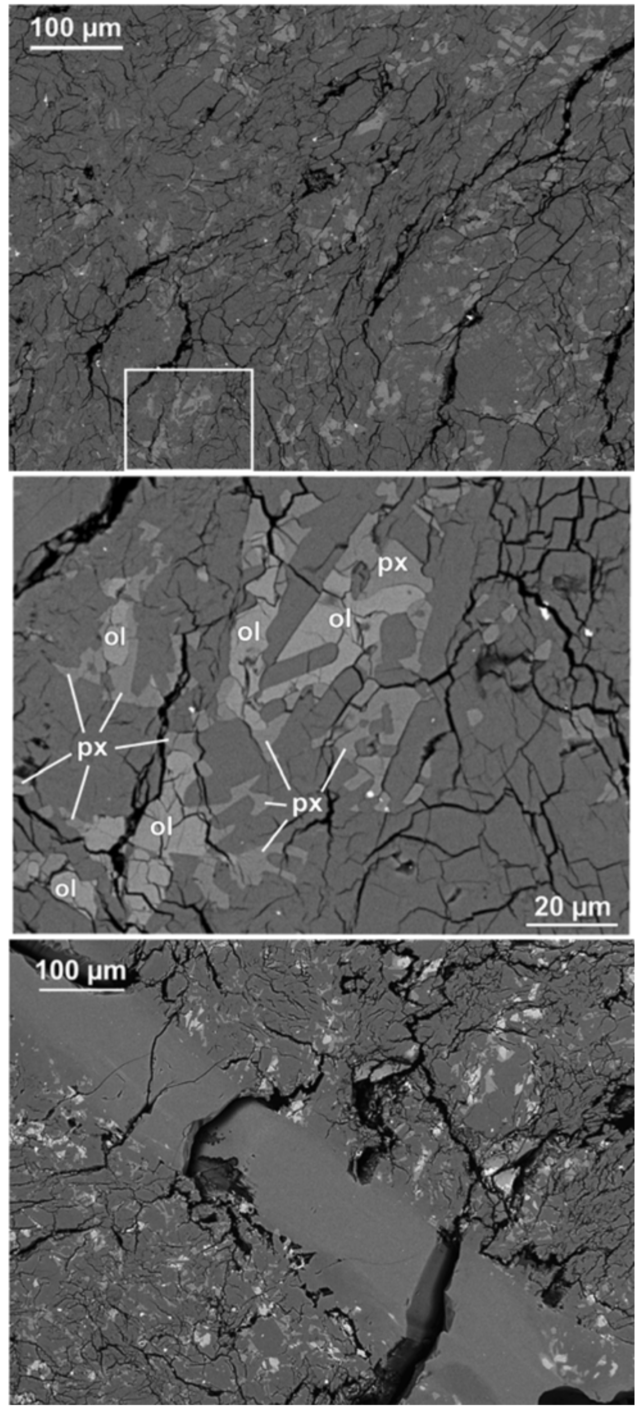

Fig. 8. Backscattered electron images of impact-melt breccia NWA 482: The texture shown in (a) and (b) is typical, except (b) is an uncommonly mafic area. In (c), a vein of shock-melt (glass) cuts through an otherwise typical region. The dark splotch along left-center margin of the vein may be a rare example of a terrestrial weathering effect in NWA 482.

formational (e.g., condensation/volatilization) processes. Three such ratios are Fe/Mn, Ga/Al, and Na/Al, probably because Mn, Ga and Na are more volatile than Fe and Al, yet within the lunar crust, Mn closely follows Fe in concentrating

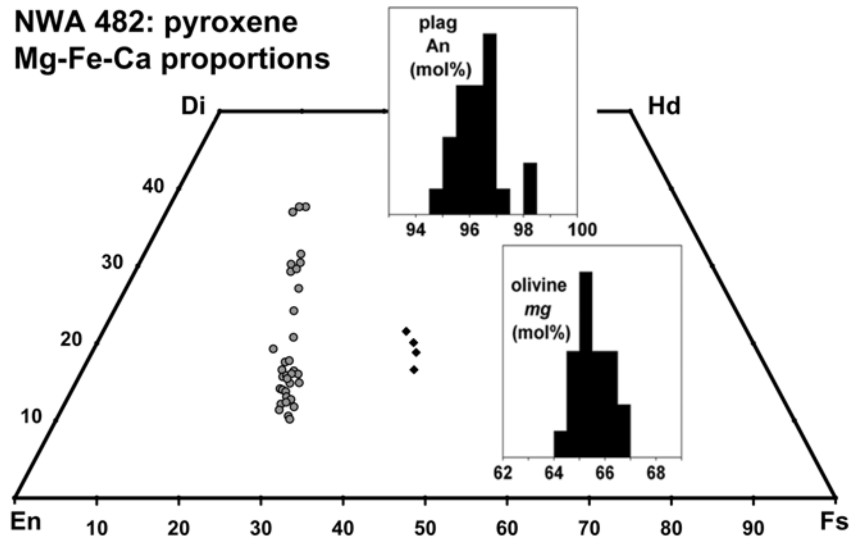

Fig. 9. A summary of compositional variations in NWA 482 minerals. The four-pyroxene analyses at anomalously high mg are all from a single small grain, situated in an otherwise nondescript region of the breccia matrix.

into mafic silicates and ilmenite, while Ga and Na closely follow Al in concentrating into plagioclase. In combination, these ratios clearly separate the new lunaites, along with other lunar materials, from all other differentiated-crustal meteoritic materials (Fig. 10). For Fe/Mn, this trend is also manifested by phase (e.g., pyroxene) FeO/MnO ratios, including our new results for several samples.

CLASSIFICATION AND ORIGIN OF DHOFAR 026

Dhofar 026 has an unusual and difficult to classify texture. Its distinctive globules were originally (Cohen et al. 2001) viewed as relicts of an earlier generation of fine-grained, mafic impact-melt breccia, set in an impact-melt breccia groundmass. Cohen et al. (2004) reinterpreted the rock as a product of impact reheating of a granulitic breccia (or possibly a fragmental breccia that consisted dominantly of granulitic breccia) and the globules as uncommonly round members of a larger population of localized melt pockets. This revised interpretation assumes that melting was limited to scattered pyroxene-rich (and thus readily melted) zones and was only indirectly caused by impact, heat having diffused from shock-melt either coating or injected into the rock. In our view, however, some details of the texture and composition of the globules are difficult to reconcile with a reheated granulitic breccia model.

Cohen et al. (2004) suggested that the round globule shapes were either inherited from clasts within a granulitic precursor rock or resulted from flow of "surrounding plagioclase glass during melting to accommodate the melt bodies." However, a shape-inheritance model does not explain how well-rounded clasts could have survived first through granulite and later through high-shock metamorphism. Granulite metamorphism by definition entails textural equilibration during slow annealing. Many of the globules consist largely of huge, almost ideally round vesicles, often near the globule margin (Figs. 4a–c). Growth of such large vesicles contemporaneously with localized melting (Cohen et al. 2004) would have required gross deformation of the original shape of the clast as well as of the surrounding plagioclase/maskelynite. The plagioclase-glass flow model also seems problematic. The model requires highly spherical vesicles to survive within virtual contact of globule margins supposedly molded by pressure from external glass flow (Figs. 4a–c), and for angular mafic grains to survive in near-contact with ovoid globule margins (Fig. 4b; cf. Fig. 2f of Cohen et al. 2004). Also, if fluidization (or lack thereof) of the surrounding plagioclase determined the degree to which mafic-melt clots became rounded, we might expect to find the spherules clustered into favorably fluidized regions of the rock. No such clustering is observed.

In the reheated granulitic breccia model (Cohen et al. 2004), the globules differ from other, more abundant types of melted mafic clots (the pyroxene-plagioclase intergrowths), but only because they happened to be molded during external plagioclase-glass flow, or possibly because they were already round. Many of the globules could only have formed by the melting of virtually an entire mafic clot, because in some cases the only visible adjacent matter is near-monomineralic plagioclase. But lunar granulitic breccias have near-uniform mafic silicate compositions (Bickel et al. 1976; Lindstrom and Lindstrom 1986). Thus, globules formed by indiscriminate whole-mafic-clot melting should have mg similar to the bulk rock, or at least to the supposedly analogous, except non-ovoid, pyroxene-plagioclase intergrowths. As discussed above, the real globules are

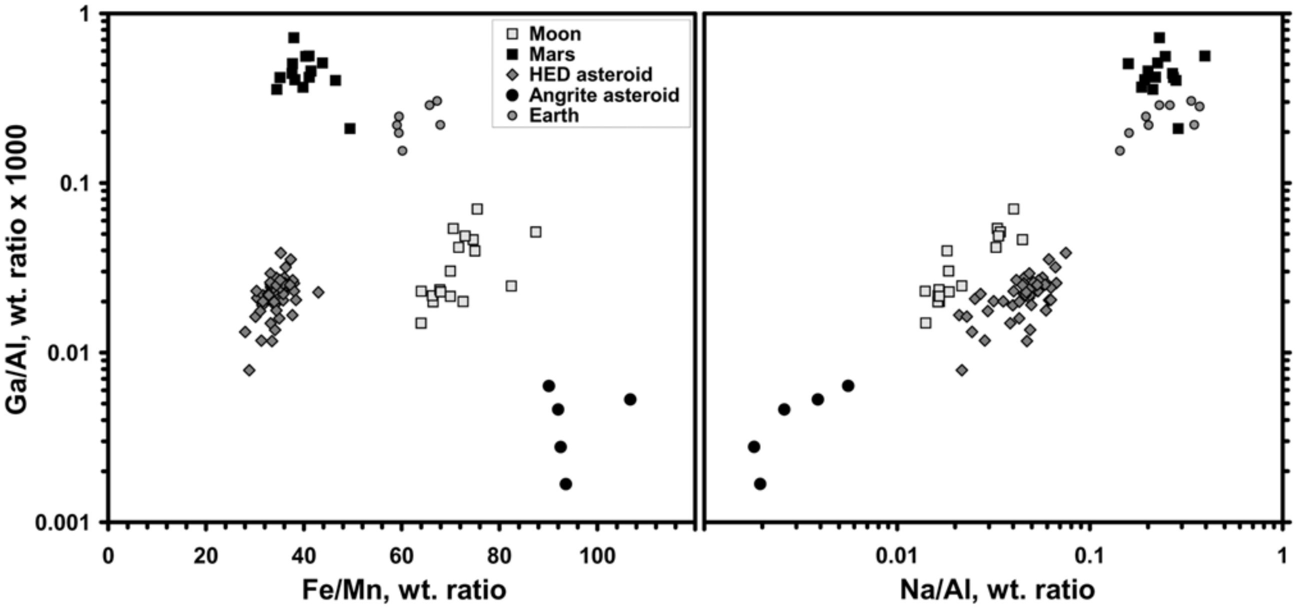

Fig. 10. In combination, bulk rock Na/Al versus Ga/Al and, Fe/Mn versus Ga/Al in particular, distinguish lunaites (and lunar samples in general) from all other planetary materials, thus confirming lunar origin.

distinctly ferroan (and sodic) in comparison to the rest of Dhofar 026, and to the pyroxene-plagioclase intergrowths in particular.

The reheated granulitic breccia model also implies a curious shock-thermal history. The 1.1-kg Apollo rock cited as analog, 15418, is grossly heterogeneous in texture (Nord et al. 1977; Ryder 1985; Cohen et al. 2004). The total mass of the recovered 13 Dhofar 026 stones (0.69 kg) is presumably but a small fraction of the original, preatmospheric meteoroid. Original separations between these samples probably exceeded the maximum dimension (15 cm) of 15418. Yet, apart from the scattered shock veins, texture is quite uniform throughout Dhofar 026. In terms of the Cohen et al. (2004) model, this means uniformity of processing, in three stages: 1) enough shock to erase a former granulitic texture, yet not enough to produce impact-shock melt, except very locally—in contrast, the entire core region of 15418 preserves a decidedly granulitic-granoblastic texture (Nord et al. 1977; Cohen et al. 2004); 2) post-shock diffusional heating, yielding T close to 1200 °C, so as to induce localized pyroxene-associated melting, but not general anatexis; and finally 3) cooling rapid enough to avoid subsequent regeneration of an annealed, granulitic texture. Uniform diffusive heating and cooling requires low thermal gradients (in relation to the decimeter-plus sampled zone). But in that case, metamorphism would have been slow and prolonged, and the most likely textural outcome would be at least mildly granulitic. The final, observed texture of Dhofar 026 is hard to classify, but clearly not granulitic.

In our opinion, the petrogenesis of Dhofar 026 remains enigmatic. Cohen et al. (2004) supplied many salient observations, but their petrogenetic model seems oversimplified. As for whether Dhofar 026 is better classified as a shocked granulitic breccia or an impact-melt breccia, French (1998) defined impact-melt breccia as having "typically" 25–75% melt and ">50–75" vol% cold rock fragments; "as the melt component increases" impact-melt breccia "grades into impact-melt rock" (cf. Simonds et al. 1976). In our opinion, the degree to which Dhofar 026 was ever granulitic is very unclear, as is how much of Dhofar 026 was, in its most intense texture-modifying event(s), directly impact-melted, and also how much of it was, after "only" absorbing an intense shock, immediately thereafter heated to the point of melting by diffusion from superheated "real" shock-melt.

If we were to adopt the Cohen et al. (2004) approach of classifying Dhofar 026 as an exceptionally shocked variety of one of the "normal" lunar rock types (Stöffler et al. 1980), we might choose immature regolith breccia as the most likely precursor rock type. The only process known to produce ovoid crystalline globules on the fluid-poor Moon is crystallization of impact-melt-droplet ejecta during ballistic transport: the "crystalline lunar spherules" (CLS) (Symes et al. 1998). CLS apparently seldom penetrate far upon landing because they occur almost exclusively in regolith breccias (e.g., Fig. 2; cf. Keil et al. 1972; King et al. 1972; Kurat et al. 1972; Ivanov et al. 1976). Symes et al. (1998) found that Apollo 14 CLS average ~0.21 ± 0.10 mm in diameter. The ovoid globules in Dhofar 026 similarly average about 0.20 ± (1σ) 0.05 mm in equivalent diameter (Cohen et al. 2004, reported average "across" dimension of 0.12 mm, but their globules category included clasts far from ovoid in

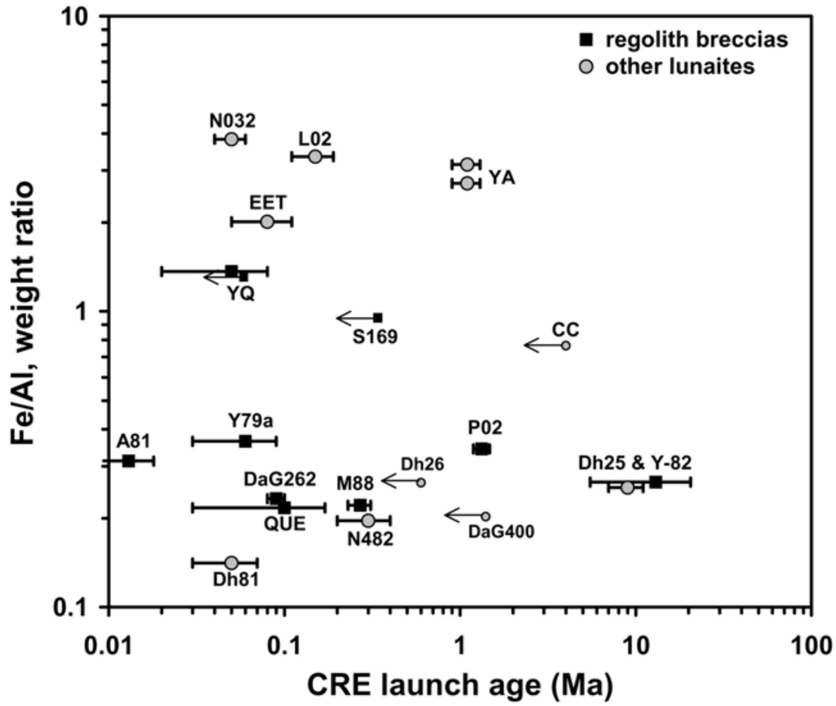

Fig. 11. A summary of CRE-constrained launch ages of lunar meteorites. In order of increasing Fe/Al, the regolith breccias are QUE 93069/94269, MAC 88104/5, DaG 262, Dhofar 025, ALH 81005, PCA 02007, Y-791197, Calcalong Creek, and Y-793274/981031; the "other" samples are fragmental breccia Dhofar 081, impact-melt breccia NWA 482, fragmental breccias Y-82192, and EET 87521, and mare basalts Y-793169, Asuka-881757, LAP 02205, and NWA 032; the upper limits are for DaG 400, Dhofar 026, SaU 169, and QUE 94281. Data are mainly from reviews by Nishiizumi et al. (1996) and Polnau and Eugster (1998); supplemented by Lorenzetti and Eugster (2002), Nishiizumi et al. (1998, 2002, 2004), Nishiizumi and Caffee (2001), Scherer et al. (1998), Swindle et al. (1995), Benoit et al. (1996), Gnos et al. (2004), and K. Nishiizumi (personal communication; especially for the two newest lunaites, LAP 02205 and PCA 02007).

shape). The sole known precedent for CLS in a non-regolithic breccia is Apollo 16 rock 63555, a vuggy-vesicular impact-melt breccia that contains a small proportion of clasts "with rounded corners" (Ryder and Norman 1980; note the Dhofar 026-globule-like clast in their Fig. 2). However, our own studies of thin section 63555,6 indicate that globule-like clasts are highly exceptional in 63555. The minor but widespread presence of CLS in Dhofar 026 (at least 11 out of 13 stones) suggests that its matrix might originally have been a regolith. If so, then for compositional purposes, Dhofar 026 might essentially be a regolith breccia. As a caveat, however, vesicles (Figs. 4a–c) are rare among Apollo/Luna CLS. Also, a shock/impact melting event would have to have thoroughly depleted noble gases from the regolithic groundmass: noble gas concentrations are lower in Dhofar 026 than in even immature regolith samples (e.g., MAC 88105) by a factor of more than 10 (Shukolyukov et al. 2001).

It is tempting to shirk classification and simply label Dhofar 026 "high-shock unique." However, considering the evidence for an important melt component and the strong likelihood that an impact was the proximal, if not instantaneous, cause of this melting, we classify this sample as an unusual variety of impact-melt breccia.

PAIRING ISSUES

Conventional (Earth-Atmosphere-Encounter) Pairing

It has long been known that QUE 93069 and QUE 94269 are paired. Pairing between Y-981031 and Y-793274 is confirmed by cosmic ray exposure (CRE) evidence (Lorenzetti and Eugster 2002). As discussed above, the 12 Dhofar stones found by the Labennes are clearly paired with Dhofar 026. However, no other cases of conventional pairing are manifest for the samples of this study. Scherer et al. (1998) asserted that DaG 262 and DaG 400 are not paired, although the deep-space ("4π") CRE of DaG 400 is loosely constrained, and the non-pairing inference seems based mainly on disparate noble gas contents (conceivably, a heterogeneous lunaite could contain noble gas-poor impact-melt breccia mingled with gas-rich regolith breccia). Data for the Dhofar lunaites (Shukolyukov et al. 2001; Nishiizumi and Caffee 2001; Nishiizumi et al. 2004) indicate that Dhofar 025 was launched from the Moon at least 5 Ma ago, whereas Dhofar 081 was launched roughly 0.04 Ma ago (Nishiizumi et al. 2004), and the launch age of Dhofar 026 is very probably <1 Ma (4π CRE lasted only 10^4 years, and a

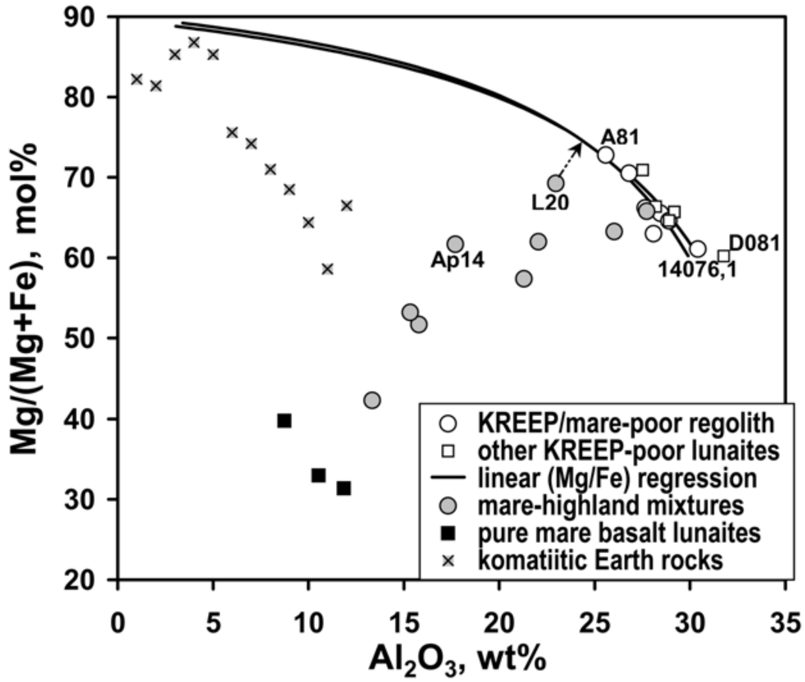

Fig. 12. Al_2O_3 versus mg. The data set used for KREEP-poor highland regoliths comprises lunaite breccias ALH 81005, DaG 262, Dhofar 025, MAC 88105, and QUE 93069, Apollo 14 sample 14076,1 (Jerde et al. 1990), and average Apollo 16 station 11 regolith (Korotev 1981). The other KREEP-poor lunaites are DaG 400, Dhofar 026, Dhofar 081, NWA 482, and Y-82192. The mare-highland mixture lunaites shown are EET 87521, PCA 02007, QUE 94281, Y-793274, and Y-983885. The pure mare basalts are Asuka-881757, NWA 032, and Y-793169. Data for komatiitic rocks from BVSP (1981). For the Luna 20 regolith, which contains about 10% mare basaltic debris, an arrow indicates extrapolation to the pure highland component. Also shown are two linear regressions, made using Mg/Fe (instead of mg) for the y-axis; in one case (the steeper trend) using only the regolith samples.

terrestrial age >0.6 Ma would be unprecedented for any stone meteorite from a hot desert). From the standpoint of available CRE constraints, Dhofars 026 and 081 might in principle be paired. However, petrographically the many Dhofar 026 stones are all highly alike, and clearly distinct from Dhofar 081. Many additional Dhofar highland lunaites (Dhofars 280, 302, 303, 305, 306, 307, 309, 310, 489, and 490) described variously as fragmental or impact-melt breccia (e.g., Nazarov et al. 2002; Takeda et al. 2004) are potentially paired with Dhofar 081. Nazarov et al. (2004) argue that Dhofars 311, 730, and 731 are a distinctly magnesian impact-melt breccia.

Launch (Source-Crater) Pairing

Before we can interpret the data for lunaites as constraints on the Moon's global surface composition, we must assess the extent to which launch pairing may be supplying us with multiple lunaites from a few common source craters. The most advantageous scenario, for our purposes, would be derivation of each lunaite from its own unique source crater.

Generic (Populational) Constraints

Cosmic ray exposure constraints (Nishiizumi et al. 1996, 2004; Polnau and Eugster 1998) are summarized in Fig. 11. On a case-by-case basis, launch pairing among lunaites is usually difficult to disprove with CRE data, because for most lunaites the trip from Moon to Earth takes well under 10^5 years (Gladman et al. 1996), and the precision of a CRE age determination is typically on the order of 10^4 to 10^5 years. As we shall see, however, CRE data have implications for source-crater pairing beyond what might be inferred by simply checking Fig. 11 for overlaps of launch-age error bars.

In Fig. 11, regolith breccias are distinguished with special symbols. Much more than other lunar rock types, regolith samples (soils and breccias) tend to show limited compositional diversity within any small region of the Moon (Warren 1994). Their compositions tend to closely follow the average composition of the underlying crust, albeit always dampened, in a statistical way, by contributions from more distant sources, which means we can be confident that two regolith breccias of grossly disparate composition (e.g., as an extreme example, pure mare versus pure highland) did not derive from a single source crater. It should also be borne in mind that the fertile region from which lunaites are launched is a small subvolume of the final launch crater (Warren 1994).

The data summarized in Fig. 11 indicate that, out of 20 partly constrained discrete launch ages, at least 3 and conceivably as many as 6 are older than 1 Ma; at least 6 and

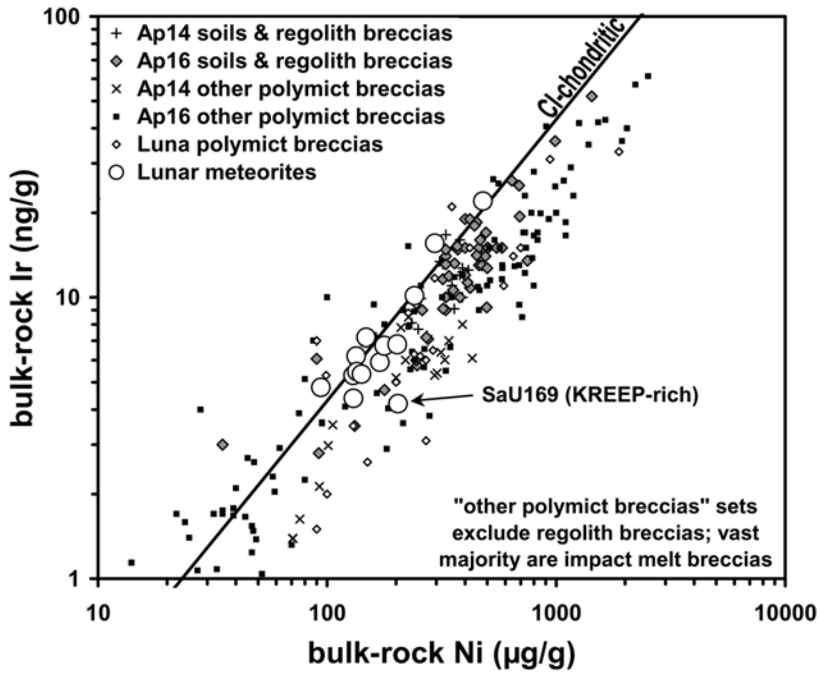

Fig. 13. Ni versus Ir in polymict breccia lunaites, polymict breccias from the two prime Apollo highland sites, and polymict breccias from Luna 16 and 20. Lunaite data are mainly from Table 1; other recent sources include Gnos et al. (2004) and Warren and Bridges (2004). Apollo sample data are from the compilation of Haskin and Warren (1991). Luna sample data are from Smith et al. (1983), Swindle et al. (1991), and Ganapathy et al. (1973).

conceivably as many as 12 are older than 0.1 Ma. The high frequency of old launch ages is significant, because using precise numerical integration of orbital evolution of model lunar ejecta, Gladman (1996; cf. Gladman et al. 1996) found that the long-term lunaite launch age spectrum should include only about 9–12% with launch ages >1 Ma, and only about 22–33% with launch ages >0.1 Ma. Thus, the observed frequencies of 15% (at least) launches older than 1 Ma, and 30% (at least) older than 0.1 Ma, are inconsistent with the expected long-term CRE age spectrum unless there are very few source-crater pairs among the lunaites with younger launch ages (cf. Korotev et al. 2003a).

As discussed by Gladman (1996), the only plausible scenario to engender a high incidence of source-crater pairing would be if an extraordinarily large impact fortuitously occurred on the Moon in the recent past (i.e., to account for the CRE data, the past 10^5 years). If that were the case, we would expect to see the total number of lunaites (currently ~30) greatly exceed the total number of martian meteorites (also currently ~30). Moreover, as reviewed by Warren (1994), "2π" CRE constraints show that most of the available lunaites were launched from shallow depths (6 out of 8 from <3 m, and 4 out of 8 from ≤1 m), as expected if most derive from relatively small craters. This tendency toward shallow launch depth, which is little-changed by more recent lunaite data (same sources as for Fig. 11), is in marked contrast to the situation with martian meteorites (none of which show any evidence for 2π exposure) (Schnabel et al. 2001), and is further confirmation that the recently launched lunaites did not come from just a few exceptionally large craters.

Specific (One-on-One) Constraints

This is not intended to be an exhaustive discussion; the emphasis will be on the newer (DaG, Dhofar, and NWA) lunaites. As suggested by Fig. 11, the CRE constraints are broadly consistent with launch pairing between Dhofar 025 and Y-82192. It is irrelevant that Dhofar 025 is a regolith breccia and Y-82192 is a fragmental breccia—in principle, they could have been over a kilometer apart on the Moon and yet end up as a launch pair. Compositionally, they are similar enough (e.g., similarly low concentrations of incompatible elements). More and better CRE constraints for Dhofar 025 might prove interesting.

DaG 400 and Dhofar 026, for which only the upper limits are available as launch age constraints, are compositionally similar enough to one another and to numerous recent-launch-age lunaites to, in principle, belong to a launch pair. NWA 482 could, in principle, be launch paired with DaG 400, Dhofar 026, MAC 88105, or (less likely) Calcalong Creek. Dhofar 081 could, in principle, be launch paired with QUE 93069/94269 and several others. In any event, as discussed above, there are strong reasons to doubt that launch pairings are common among the lunaites of recent launch age.

WEATHERING ISSUES

Nearly all of the warm desert lunaites (DaG, Dhofar, and NWA) show clear signs of compositional alteration by terrestrial weathering. The only major exception is NWA 482. Of the elements determined (Table 1), one of the most sensitive to alteration is Sr. Unaltered lunar materials rarely have Sr >200 µg/g (Haskin and Warren 1991), but 5 of our 12 Dhofar 026 samples have Sr >500 µg/g. Other alteration-sensitive elements include Ba and U, alterations of which manifest as Ba/La and Th/U ratios far from the KREEP values of 12 and 3.6, respectively (Warren 2004), and Sb, which is normally <20 ng/g. Most of the same lunaites that show enhanced Sr also show enhanced Sb. Despite relatively normal Sr, DaG 400 shows greatly enhanced Ba/La and a particularly strong U enhancement. Many samples also show Au/Ir ratios greatly enhanced over the chondritic value (0.3). But routine handling (gold jewelry) can easily engender Au contamination, and these samples may have been much-handled before we acquired them; so the Au/Ir enhancements may be artificial.

Even though all of the Dhofar 026 samples are significantly weathered, comparison of the different Dhofar 026 results suggests that for many incompatible and siderophile trace elements, weathering has had little effect. Dhofar 468, which has grossly contaminated Sr and Ba and suspiciously high Sb, nonetheless is near-average in terms of REE, Th, and other incompatible elements, and unexceptional in terms of Ni and Ir. Also, as discussed above, correlations between incompatible elements and Fe have survived among the Dhofar 026 samples. In general, except for Cs, Ba, and U, incompatible element patterns of the hot desert samples, including the two DaG lunaites and NWA 482, conform well to the classic KREEP pattern so typical of lunar highland materials (Warren 2004). Apparently, despite the susceptibility of Cs, Ba, and U (and Sr and Sb), most of the highly incompatible elements are resistant, in lunaites, to major bulk-rock alteration by warm desert weathering. The same conclusion has been drawn previously, particularly with respect to Th, by Bischoff et al. (1998) and Fagan et al. (2001).

MAJOR ELEMENT TRENDS: THE HIGHLAND Mg-RICH COMPONENT

An interesting trend is manifested by highland polymict breccia lunaites and KREEP-poor Apollo/Luna highland regolith samples on a plot of Al_2O_3 versus mg (Fig. 12). In this figure, samples that contain significant KREEP or mare components are distinguished from the KREEP-poor highland samples with grey symbols. With ~20 wt% FeO and ~10 wt% Al_2O_3, mare basalt admixture can markedly shift the locus of a highland polymict breccia on an Al_2O_3 versus mg plot. KREEP basalts also feature relatively low mg and Al_2O_3 (e.g., Warren 1988). Regolith breccias are distinguished for emphasis. As lithified soils, regolith breccias are products of extremely thorough blending of debris from countless predominantly local crustal rocks. As each regolith sample is essentially a product of natural averaging of the nearby crust, regolith breccias tend to show only limited compositional diversity, compared to the mélange of igneous rocks at any given locale (e.g., McKay et al. 1986, 1989).

Evidence for a large mare component in the Luna 20 regolith and a significant one in Y-791197 was reviewed by Simon et al. (1981) and Warren (1994), respectively. In the case of Luna 20, sufficient data are available to constrain the magnitude of the mare component to be 10 wt% ± ~2 wt% of the soil. The mare component is 7–8 wt%, based on data for >90 µm lithic fragments (finer fractions have slightly higher mafic/plagioclase ratios), or 11–12 wt%, based on data for glasses (Simon et al. 1981; Snyder et al. 1999; Cohen et al. 2001; and many references cited by Warren 1994). Assuming a 10 wt% mare component compositionally equivalent to an average of Luna 16 and Luna 24 mare basalts (Arai and Warren 1999), extrapolation to the pure highland composition implies Al_2O_3 ~24.3 wt% and mg ~74.3 mol% (cf. Korotev 2002), in excellent agreement with extrapolation of the anticorrelation defined by the highland polymict breccia lunaites and other KREEP-poor highland regolith samples.

The KREEP-poor highland samples show a significant (r = 0.90) trend of increasing mg with decreasing Al_2O_3. This trend tends to confirm that the same main petrologic ingredients are present in the crust as a whole as in the Apollo 16 region: ferroan anorthosite, with high Al_2O_3 and low mg, and a component that is both less anorthositic and more magnesian (e.g., Warren 1990). The most magnesian member of the trend (ALH 81005) presumably does not represent the end-member magnesian component because the anorthositic component that is so ubiquitous elsewhere in the lunar highlands (based on general geological constraints, and Clementine global FeO data in particular: Lucey et al. 1995) might be low, but can hardly be absent in a mature regolith breccia like ALH 81005.

The magnesian component conceivably formed as magnesian (earlier, and/or less trapped-melt-rich) flotation cumulates from the same magma ocean that engendered the ferroan-anorthositic component. But there are severe problems with such a model. The ferroan-anorthositic component has been sampled in the form of numerous pristine (compositions virtually unaltered since origin by endogenous magmatism: Warren and Wasson 1980a; Warren 1990) cumulates, including some with relatively high mafic contents. The mafic silicates within the ferroan-anorthositic component are clearly not associated with the higher levels of incompatible element contents that would be commensurate with the presence of more than a tiny fraction of trapped melt (Warren and Wasson 1980a). Thus, the magnesian crustal component cannot be comagmatic with the ferroan-anorthositic component, unless it formed at a much earlier stage of the magma's crystallization. On diagrams of mg versus a plagiophile ratio such as Eu/Al, the ferroan-anorthositic pristine rocks form a tight cluster separated from all others by a large gap, implying a thoroughly distinct petrogenesis (Warren and Kallemeyn 1984). Models of feldspathic crust flotation over a crystallizing magma ocean (Warren 1990) imply that melt density increases as FeO concentration increases during crystallization. The melt is saturated in pyroxene (and generally also olivine) as well as plagioclase, and the nascent crust tends to entrain a proportion of these mafics, or melt that promptly crystallizes mafics. But the efficiency of this entrainment is sensitive to the density differences among the phases, especially between the melt (which all the while grows increasingly dense) and the sole buoyant solid, plagioclase (Warren 1990). As a result, the proportion of mafic silicates in the nascent flotation crust should generally increase during the crystallization sequence. Thus, the trend among the KREEP-poor highland samples on Fig. 12 would be expected to show just the opposite slope, Al_2O_3 decreasing with decreasing mg, if the magnesian component formed as earlier flotation cumulates from the same magma ocean that engendered the ferroan-anorthositic component.

The magnesian component is conceivably upper mantle material ejected from a giant basin (South Pole–Aiken would be the most obvious candidate; the site must be far from the KREEP-rich Procellarum region). In that case, the trend of Fig. 12 would extrapolate to an extremely low Al_2O_3 and extremely high mg. For example, assuming a conservatively high Al_2O_3 for the upper mantle, say 5 wt%, the extrapolated mg would be 88–89 mol%.

More probably, the magnesian component is crustal, and specifically represents the chemical signature of the Mg-suite of pristine nonmare rocks, or rather, of a "pure" Mg-suite component within the overall Mg-suite; "pure" in the sense that it that managed to avoid the major assimilation/mixing with KREEP that is so common among Apollo Mg-suite samples (e.g., Warren 1988; Shearer and Papike 1999). The inference of such a high mg for the lunar highland magnesian component has important implications for estimates of the bulk composition of the Moon, as discussed in this paper's companion (Warren 2005).

In Fig. 12, the ferroan end of the KREEP-poor highland trend is defined by a ferroan anorthositic component that is of course itself a mixture of diverse individual ferroan anorthositic rocks, which even among the limited number of Apollo samples range from nearly pure plagioclase rocks to anorthositic norites and troctolites. The average composition and especially the average plagioclase (i.e., Al_2O_3) content of the ferroan suite rocks is of great interest because this rock type dominates the lunar crust and because its high modal plagioclase is a key aspect of, and a prime justification for, the magma ocean hypothesis (e.g., Warren 1990). A defining characteristic of the ferroan anorthositic suite is that its members, and especially its members with significant proportions of MgO and FeO, seldom have bulk mg far from 60 mol%. Assuming that ferroan-anorthositic material averages mg ~60 mol%, the regression trend in Fig. 12 suggests that its average Al_2O_3 ~29–30 wt% (implying about 14–15 vol%, or 17–19 wt%, modal mafic silicates). However, two potential complications should be noted. First, Warren's (1990) magmasphere crystallization model suggests that as the ferroan-anorthositic flotation crust thickened, its modal mafic content tended to increase in response to increasing melt density. If so, mafic content may increase with depth in the final crust. The impact-excavation process that mixed the ferroan-anorthositic matter into the available samples is biased toward shallow crust, so the samples may be biased toward high Al_2O_3. However, there must also be a slight bias toward low Al_2O_3, because even the samples classed as KREEP-poor and mare-free in Fig. 12 are thoroughly polymict breccias that probably, and in most cases definitely (e.g., Warren 1994) contain small proportions of both KREEP and mare basalt. In any case, the inferred mafic content of 17–19 wt% agrees well with Warren's (1990) model result of ~19 wt%, assuming that the mafic content was determined by crust/melt buoyancy relationships during flotation crust growth over a magma ocean.

SIDEROPHILE TRACE ELEMENTS

We focus in this section on Ni and Ir, in part because Au, the most siderophile among the other elements widely determined in lunaites, tends to suffer from terrestrial alteration (including artificial contamination, in these often roughly handled samples). The ratio Ni/Ir is nearly constant among chondrites; for example, 22500 ± 4200 µg/g among 11 different chondrite varieties studied by Wasson and Kallemeyn (1988) and Kallemeyn et al. (1991, 1994). Highland samples from the Apollo 14 and 16 sites tend to have surprisingly high Ni/Ir (Fig. 13), on average about 1.8× the chondritic ratio (e.g., Korotev 1987; Warren et al. 1989); similarly high Ni/Ir is also typical of Apollo 15 and 17 highland materials, albeit these are not included in our busy Fig. 13. Among Apollo 14 and 16 samples, impact melts tend to have higher Ni/Ir than regolith breccias; presumably because in regolith breccias the local siderophile signature is diluted by a "micrometeorite" component (Wasson et al. 1975).

From the Luna 20 site, far to the east of the Apollo sampling region, a suite of 14 rocklets analyzed by Smith et al. (1983) show a similar tendency toward high Ni/Ir, averaging 2.4× CI-chondritic (Fig. 13). All or nearly all of the Smith et al. (1983) samples are impact-melt breccias (unpublished petrologic study by P. H. Warren). The Smith et al. (1983) laboratory at Oregon State was known for consistent accuracy, but it should be noted that data for six

Luna 20 rocklets from Swindle et al. (1991) mostly show nearly chondritic Ni/Ir (average, 1.2× CI-chondritic). Overall, the data from Luna 20 (including an analysis by Ganapathy et al. 1973) have average Ni/Ir = 2.0× CI-chondritic.

Using lunaites, we can ask: are the high Ni/Ir ratios among samples from the central nearside (and if the Smith et al. 1983, data are accurate, also the east-central nearside) representative of the overall lunar highlands? The lunaites' answer is a resounding no (Fig. 13). The SaU 169 meteorite has an exceptionally high Ni/Ir, but this only confirms other cogent evidence (Gnos et al. 2004) that pinpoints the source crater of this extremely KREEP-rich rock on the central nearside. Among 13 other highland lunaites, average Ni/Ir is precisely chondritic at 24300 ± 3600 (ignoring our one exceptionally siderophile-rich sample of Dhofar 026, which, if included, would result in a weirdly low Ni/Ir). Most of the highland lunaites are regolith breccias, but even for the three impact-melt breccia lunaites, average Ni/Ir is chondritic at 25000 ± 3000.

Why do the central and east-central nearside highland samples have such high Ni/Ir? As noted by Warren et al. (1989), the absence of a similar composition among lunaites, including the magnesian regolith breccia ALH 81005, militates against the notion (Ringwood et al. 1987) that high Ni is an endogenous feature associated with the magnesian component of the lunar crust. Moreover, the Ni content of the lunar mantle inferred from mare basalt data (Warren et al. 1999) is about 7 times lower than the level invoked by Ringwood et al. (1987). Mantle Ni levels inferred from mare pyroclastic glasses are similar (e.g., Delano 1986) or even lower (Walker et al. 2004) than those inferred from the basalts.

Korotev (1987) suggested that two or three compositionally similar iron asteroids were the chief sources of siderophile elements at the Apollo 16 site. It seems dubious to assume that multiple compositionally similar asteroids were steered toward the Apollo 16 area. This dynamic problem is exacerbated because high Ni/Ir is also a feature of the other Apollo sites, and, it now appears, even the Luna 20 site. The distance between the Apollo 14 and Luna 20 sites is 2250 km.

The high-Ni/Ir anomaly will likely remain enigmatic until a far more comprehensive sampling of the Moon is achieved. In the meantime, we can only speculate that it reflects dominantly the siderophile component deposited, heterogeneously, from a single exceptionally large central nearside impact. However, no single, clearly surviving impact basin is positioned where it would be expected to dominate the late-accretionary component at all the known high-Ni/Ir sites (the Apollo 16 site, in the middle of the high-Ni/Ir anomaly, is about as far from any large, recognizable basin as a nearside site can be).

The notion that a uniform siderophile signature is left by any single impact is probably an oversimplification. Impacts are frequently oblique, and impactors large enough to create a lunar basin (i.e., asteroids of order 100 km in diameter) are probably frequently differentiated. The distal ejecta from such an event might feature quirks inherited from one side, and/or one radial level, within the impactor. Moreover, volatilization-condensation processes can lead to siderophile heterogeneity even in a single relatively small impact (Mittlefehldt and Hörz 1998). The only obvious candidates for the role of heterogeneous impactor are the impactor(s) that created Imbrium and, possibly, Procellarum. Schultz (1995) suggested that both the Imbrium basin and the concentric structures attributed to a Procellarum impact formed by a single oblique impact from the northwest. In terms of modeling the enigmatic high-Ni/Ir anomaly of the Apollo-Luna region as the vestige of an oblique Imbrium impact, a trajectory from the northwest would be favorable for spewing the anomaly to the great distance of the Luna 20 site, 2280 km. Of course, the coincidence of high Ni/Ir at all of the central and east-central nearside highland sites might conceivably be just that: a coincidence produced by 2–3 impacts sharing the same compositional quirk; as Korotev (1987) invoked, albeit for Apollo 16 only.

COMPARISON BETWEEN LUNAITE AND APOLLO/ LUNA IMPACT-MELT BRECCIAS

The two lunaite impact-melt breccias, or three if the impact-melt dominated DaG 400 is included, are all highly anorthositic by the standards of impact melts from the limited Apollo sampling region (Fig. 6). Even taking this into account, the lunaite IMBs are also KREEP-poor. On average, the three lunaite IMBs contain only ~ 0.17× as much Sm and 0.13× as much Th as the average composition of the three similarly anorthositic Apollo 16 impact melt groups (Morris et al. 1986; Korotev 1994). Extrapolation to the Dhofar 026 typical globule composition (Table 2) suggests the globule impact melt, too, was uncommonly KREEP-poor in comparison to analogously mafic Apollo impact-melt breccias (Fig. 6). This type of disparity between the lunaite and Apollo IMB populations is no great surprise, because an analogous pattern was noted previously from comparison between lunaite and Apollo regolith breccias (Warren and Kallemeyn 1991). Remote-sensing data have shown that the Apollo region is unrepresentatively KREEP-rich (Lawrence et al. 2003). Evidently, the KREEP component, so pervasively blended into the Apollo 16 samples (albeit all-important in terms of incompatible trace elements), does not greatly dampen major-element compositional diversity.

Data for Luna 20 and two anorthositic Luna 16 IMBs are also included in Fig. 6. Despite great scatter (individual rocklets are shown, as opposed to group averages for the Apollo samples; most of the analyzed rocklets weigh less than 2 g), the Luna samples from the eastern central nearside in general show similar Al_2O_3—incompatible element trends as the lunar meteorites. Again, the Apollo 16 samples appear unrepresentatively rich in KREEP (Th, Sm, etc.) compared to the overall lunar surface.

CONCLUSIONS

Several of the "newest" highland lunaites of this study, DaG 400, Dhofar 026 and Dhofar 081, are difficult to classify. On balance, Dhofar 081 appears to be a fragmental breccia, but much of its groundmass features a glassy-fluidized texture indicative of localized shock melting, so it might arguably be classified as an impact-melt breccia. As a further complication, swirly brown glass, which is common in the glassy-fluidized matrix of Dhofar 081, is suggestive of a regolith derivation. DaG 400 is a regolith breccia, but its constituent clasts comprise preponderantly anorthositic impact-melt breccias. Dhofar 026 is an unusual type of anorthositic impact-melt breccia with a widely dispersed smattering of mafic, subophitic, and possibly relict, impact-melt globules. The presence of mafic crystalline globules in a lunar material, even one so profoundly impact-heated, suggests that it may originally have been a regolith. NWA 482 is a relatively straightforward impact-melt breccia.

The KREEP component that dominates the incompatible trace element compositions of Apollo (central nearside) highland samples, although relatively minor in a volumetric sense, probably played an important role in petrogenesis of the sampled (Apollo) Mg-suite pristine nonmare rocks (e.g., Warren 1988; Shearer and Papike 1999; Korotev 2000; Jolliff et al. 2000; Wieczorek and Phillips 2000). But the notion that the only magnesian component in the upper crust is associated with the central nearside's KREEP (Korotev 2000) is called into question by a strong anticorrelation between Al_2O_3 and mg that we find manifested by KREEP-poor highland samples. This trend indicates that the upper crust as a whole is dominated by the same main petrologic ingredients that dominate in the Apollo 16 region: ferroan anorthosite with high Al_2O_3 and low mg, and a component that is less anorthositic and more magnesian. The magnesian component in the KREEP-poor samples may represent the chemical signature of the Mg-suite of pristine nonmare rocks, in its most pure form, unaltered by the major KREEP-assimilation that is so common among Apollo Mg-suite samples. The inference of such a high mg for the lunar highland magnesian component has important implications for estimates of the bulk composition of the Moon (Warren 2005). The average composition of the ferroan anorthositic component is now well constrained at Al_2O_3 ~29–30 wt% (implying about 14–15 vol%, or 17–19 wt%, modal mafic silicates), in good agreement with the composition predicted for flotation crust over a "ferroan" magma ocean (Warren 1990).

Our new data and a synthesis of literature data manifest a contrast in Al_2O_3-incompatible element systematics between impact melts from the KREEP-rich central nearside highlands, where Apollo sampling occurred, and those from the general highland surface of the Moon, as represented by impact-melt breccias among the lunaites, and also Luna samples. Even the mafic globules within Dhofar 026 are inferred, based on extrapolation from whole-rock trends, to be much less KREEP-rich than typical Apollo samples of similar Al_2O_3 concentration.

Siderophile elements also show a distinctive composition prevalent among Apollo impact-melt breccias: Ni/Ir averaging about twice chondritic. In contrast, lunaite impact-melt breccias have consistently chondritic Ni/Ir. In this case, unlike the lunaites, highland impact melts from the Luna sites show similarity (i.e., generally high Ni/Ir) with the Apollo samples. The prevalence of this distinctive Ni/Ir ratio at such widely separated nearside sites suggests that debris from one extraordinarily large impact may dominate the siderophile component of the megaregolith in a nearside region 2300 km or more across.

Acknowledgments–For generous allocations of samples, we wish to thank NSF, the Meteorite Working Group, and the Japanese NIPR (for Antarctic meteorites), M. A. Nazarov and Larry Taylor (Moscow and Knoxville, for Dhofar 025 and the original Dhofar 026 stone), Jutta Zipfel (Mainz, for DaG 400), Addi Bischoff (Münster, for DaG 262), Dieter Stöffler (Berlin, for Dhofar 081), Mike Farmer (for NWA 482), and Marc Labenne (for several Dhofar 026 samples). We also thank J. Delano, O. James, and B. Jolliff for helpful reviews. This research was supported by NASA grant NAG5-4215.

Editorial Handling—Dr. David Mittlefehldt

REFERENCES

Arai T. and Warren P. H. 1999. Lunar meteorite QUE 94281: Glass compositions and other evidence for launch pairing with Yamato-793274. *Meteoritics & Planetary Science* 34:209–234.

Arai T., Ishii T., and Otsuki M. 2002. Mineralogical study of a new lunar meteorite Yamato-981031 (abstract #2064). 33rd Lunar and Planetary Science Conference. CD-ROM.

Arai T., Misawa K., and Kojima H. 2005. A new lunar meteorite MET 01210: Mare breccia with a low-Ti ferrobasalt (abstract #2361). 36th Lunar and Planetary Science Conference. CD-ROM.

Benoit P. H., Sears D. W. G., and Symes S. J. K. 1996. The thermal and radiation exposure history of lunar meteorites. *Meteoritics & Planetary Science* 31:869–875.

Bersch M. G., Taylor G. J., Keil K., and Norman M. D. 1991. Mineral compositions in pristine lunar highland rocks and the diversity of highland magmatism. *Geophysical Research Letters* 18:2085–2088.

Bickel C. E., Warner J. L., and Phinney W. C. 1976. Petrology of 79215: Brecciation of a lunar cumulate. Proceedings, 7th Lunar Science Conference. pp. 1793–1819.

Bischoff A., Palme H., Weber H. W., Stöffler D., Braun O., Spettel B., Begemann F., Wänke H., and Ostertag R. 1987. Petrography, shock history, chemical composition and noble gas content of the lunar meteorites Yamato-82192 and -82193. *Proceedings of the Eleventh Symposium on Antarctic Meteorites.* pp. 21–42.

Bischoff A., Weber D., Clayton R. N., Faestermann T., Franchi I. A., Herpers U., Knie K., Korschinek G., Kubik P. W., Mayeda T. K., Merchel S., Michel R., Neumann S., Palme H., Pillinger C. T., Schultz L., Sexton A. S., Spettal B., Verchovsky A. B., Weber H. W., Weckwerth G., and Wolf D. 1998. Petrology, chemistry, and isotopic compositions of the lunar highland regolith breccia Dar al Gani 262. *Meteoritics & Planetary Science* 33:1243–1257.

Bukovanska M., Dobosoi G., Brandstätter F., and Kurat G. 1999. Dar al Gani 400: Petrology and geochemistry of some major lithologies (abstract). *Meteoritics & Planetary Science* 34:A21.

Basaltic Volcanism Study Project. 1981. *Basaltic volcanism on the terrestrial planets*. New York: Pergamon Press. 1286 p.

Cohen B. A., Kring D. A., and Swindle T. D. 1999. Impact melt clasts in lunar meteorites Dar al Gani 262 and Dar al Gani 400 (abstract). *Meteoritics & Planetary Science* 34:A26–A27.

Cohen B. A., Taylor L. A., and Nazarov M. A. 2001. Lunar meteorite Dhofar 026: A second-generation impact melt (abstract #1404). 32nd Lunar and Planetary Science Conference. CD-ROM.

Cohen B. A., James O. B., Taylor L. A., Nazarov M. A., and Barsukova L. D. 2004. Lunar highland meteorite Dhofar 026 and Apollo sample 15418: Two strongly shocked, partially melted, granulitic breccias. *Meteoritics & Planetary Science* 39:1419–1447.

Daubar I. J., Kring D. A., Swindle T. D., and Jull A. J. T. 2002. Northwest Africa 482: A crystalline impact-melt breccia from the lunar highlands. *Meteoritics & Planetary Science* 37:1797–1813.

Delano J. W. 1986. Abundances of cobalt, nickel, and volatiles in the silicate portion of the Moon. In *Origin of the Moon*, edited by Hartmann W. K., Phillips R. J., and Taylor G. J. Houston: Lunar and Planetary Institute. pp. 231–247.

Delano J. W. 1991. Geochemical comparison of impact glasses from lunar meteorites ALH A81005 and MAC 88105 and Apollo 16 regolith 64001. *Geochimica et Cosmochimica Acta* 55:3019–3029.

Drozd R. J., Kennedy B. M., Morgan C. J., Podosek F. A., and Taylor G. J. 1976. The excess fission xenon problem in lunar samples. Proceedings, 7th Lunar Science Conference. pp. 599–624.

Elphic R. C., Lawrence D. J., Feldman W. C., Barraclough B. L., Maurice S., Binder A. B., and Lucey P. G. 2000. Lunar rare earth element distribution and ramifications for FeO and TiO_2—Lunar Prospector neutron spectrometer observations. *Journal of Geophysical Research* 105:20,333–20,345.

Fagan T. J., Taylor G. J., Keil K., Bunch T. E., Wittke J. H., Korotev R. L., Jolliff B. L., Gillis J. J., Haskin L. A., Jarosewich E., Clayton R. N., Mayeda T. K., Fernandes V. A., Burgess R., Turner G., Eugster O., and Lorenzetti S. 2001. Northwest Africa 032: Product of lunar volcanism. *Meteoritics & Planetary Science* 37:371–394.

French B. M. 1998. *Traces of catastrophe: A handbook of shock-metamorphic effects in terrestrial and meteorite impact structures*. Houston: Lunar and Planetary Institute. 120 p.

Ganapathy R., Morgan J. W., Krähenbühl U., and Anders E. 1973. Ancient meteoritic components in lunar highland rocks: Clues from trace elements in Apollo 15 and 16 samples. Proceedings, 4th Lunar Science Conference. pp. 1239–1261.

Gladman B. J. 1996. Delivery of planetary ejecta to Earth. Ph.D. thesis, Cornell University, Ithaca, New York, USA.

Gladman B. J., Burns J. A., Duncan M., Lee P., and Levison H. F. 1996. The exchange of impact ejecta between terrestrial planets. *Science* 271:1387–1392.

Gnos E., Hofmann B. A., Al-Kathiri A., Lorenzetti S., Eugster O., Whitehouse M. J., Villa I. M., Jull A. J. T., Eikenberg J., Spettel B., Krähenbühl U., Franchi I. A., and Greenwood R. C. 2004. Pinpointing the source of a lunar meteorite: Implications for the evolution of the Moon. *Science* 305:657–659.

Greshake A., Schmitt R. T., Stöffler D., Pätsch M., and Schultz L. 2001. Dhofar 081: A new lunar highland meteorite. *Meteoritics & Planetary Science* 36:459–470.

Grossman J. N. and Baedecker P. A. 1986. Computer graphics for quality control in the INAA of geological samples. Proceedings, 7th International Conference on Modern Trends in Activation Analysis. pp. 571–578.

Haskin L. A. and Warren P. H. 1991. Chemistry. In *Lunar sourcebook: A user's guide to the Moon*, edited by Heiken G., Vaniman D. and French B. M. Cambridge: Cambridge University Press. pp. 357–474.

Ivanov A. V., Nazarov M. A., Rode O. D., and Shevaleevski I. D. 1976. Chondrule-like particles from Luna 16 and Luna 20 regolith samples. Proceedings, 7th Lunar Science Conference. pp. 743–758.

Jerde E. A., Morris R. V., and Warren P. H. 1990. In quest of lunar regolith breccias of exotic provenance—A uniquely anorthositic sample from the Fra Mauro (Apollo 14) highlands. *Earth and Planetary Science Letters* 98:90–108.

Jolliff B. L., Gillis J. J., Haskin L. A., Korotev R. L., and Wieczorek M. A. 2000. Major lunar crustal terranes: Surface expressions and crust-mantle origins. *Journal of Geophysical Research* 105: 4197–4216.

Jolliff B. L., Korotev R. L., and Rockow K. M. 1998. Geochemistry and petrology of lunar meteorite Queen Alexandra Range 94281: A mixed mare and highland regolith breccia, with special emphasis on very-low-Ti mafic components. *Meteoritics & Planetary Science* 33:581–601.

Kallemeyn G. W. 1993. Neutron activation analysis. In *Advances in analytical chemistry*, edited by Hyman M. and Rowe M. W. London: JAI Press. pp. 193–209.

Kallemeyn G. W., Rubin A. E., and Wasson J. T. 1991. The compositional classification of chondrites. V. The Karoonda (CK) group of carbonaceous chondrites. *Geochimica et Cosmochimica Acta* 55:881–892.

Kallemeyn G. W., Rubin A. E., and Wasson J. T. 1994. The compositional classification of chondrites: VI. The CR carbonaceous chondrite group. *Geochimica et Cosmochimica Acta* 58:2873–2888.

Keil K., Kurat G., Prinz M., and Green J. A. 1972. Lithic fragments, glasses and chondrules from Luna 16 fines. *Earth and Planetary Science Letters* 13:243–256.

Keith J. E., Clark R. S., and Richardson K. A. 1972. Gamma ray measurements of Apollo 12, 14, and 15 lunar samples. Proceedings, 3rd Lunar Science Conference. pp. 1671–1680.

Kempa M. J. and Papike J. J. 1980. The Apollo 16 regolith: Comparative petrology of the >20 µm and 20-10 µm soil fractions, lateral transport and differential volatilization. Proceedings, 11th Lunar and Planetary Science Conference. pp. 1635–1661.

King E. A., Jr., Butler J. C., and Carman M. F. 1972. Chondrules in Apollo 14 samples and size analyses of Apollo 14 and 15 fines. Proceedings, 3rd Lunar Science Conference. pp. 673–686.

Koeberl C., Kurat G. and Brandstätter F. 1990. Lunar meteorite Yamato-86032: Mineralogical, petrological, and geochemical studies. *Proceedings of the NIPR Symposium on Antarctic Meteorites* 14:3–18.

Koeberl C., Kurat G., and Brandstätter F. 1996. Mineralogy and geochemistry of lunar meteorite Queen Alexandra Range 93069. *Meteoritics & Planetary Science* 31:897–908.

Kojima H. 2000. Some unique achondrites in the Yamato-98 meteorites (abstract). *Antarctic Meteorites* 25:55.

Korotev R. L. 1981. Compositional trends in Apollo 16 soils.

Proceedings, 12th Lunar and Planetary Science Conference. pp. 577–605.
Korotev R. L. 1987. The meteoritic component of Apollo 16 noritic impact melt breccias. Proceedings, 17th Lunar and Planetary Science Conference. pp. 491–512.
Korotev R. L. 1994. Compositional variation in Apollo 16 impact melt breccias and inferences for the geology and bombardment history of the central highlands of the Moon. *Geochimica et Cosmochimica Acta* 58:3931–3969.
Korotev R. L. 2000. The great lunar hot spot and the composition and origin of the Apollo mafic ("LKFM") impact-melt breccias. *Journal of Geophysical Research* 105:4317–4345.
Korotev R. L. 2002. The Luna 20 regolith (abstract #1224). 33rd Lunar and Planetary Science Conference. CD-ROM.
Korotev R. L., Jolliff B. L., and Rockow K. M. 1996. Lunar meteorite Queen Alexandra Range 93069 and the iron concentration of the lunar highlands surface. *Meteoritics & Planetary Science* 31: 909–924.
Korotev R. L., Jolliff B. L., Zeigler R. A., Gillis J. J., and Haskin L. A. 2003a. Feldspathic lunar meteorites and their implications for compositional remote sensing of the lunar surface and the composition of the lunar crust. *Geochimica et Cosmochimica Acta* 67:4895–4923.
Korotev R. L., Jolliff B. L., Zeigler R. A., and Haskin L. A. 2003b. Compositional constraints on the launch pairing of three brecciated lunar meteorites. *Antarctic Meteorite Research* 16: 152–175.
Kurat G., Keil K., Prinz M., and Nehru C. E. 1972. Chondrules of lunar origin. Proceedings, 3rd Lunar Science Conference. pp. 707–721.
Lawrence D. J., Elphic R. C., Feldman W. C., and Prettyman T. H. 2003. Small-area thorium features on the lunar surface. *Journal of Geophysical Research* 108:6-1–6-25.
Lindstrom M. M. and Lindstrom D. J. 1986. Lunar granulites and their precursor anorthositic norites of the early lunar crust. Proceedings, 16th Lunar and Planetary Science Conference. pp. D263–D276.
Lindstrom M. M., Marvin U. B., Holmberg B. B., and Mittlefehldt D. W. 1990. Apollo 15 KREEP-poor impact melts. Proceedings, 20th Lunar and Planetary Science Conference. pp. 77–90.
Lindstrom M. M., Mittlefehldt D. W., Morris R. V. and Martinez R. R. 1995. QUE 93069, a more mature regolith breccia for the Apollo 25th anniversary (abstract). 26th Lunar and Planetary Science Conference. pp. 849–850.
Lorenzetti S. and Eugster O. 2002. Noble gas characteristics of lunar meteorite Yamato-981031 paired with basaltic-anorthositic breccia Yamato-793274 (abstract). *Antarctic Meteorites* 27:75–76.
McKay D. S., Heiken G., Basu A., Blanford G., Simon S., Reedy R., French B. M., and Papike J. 1991. The lunar regolith. In *Lunar sourcebook: A user's guide to the Moon*, edited by Heiken G., Vaniman D., and French B. M. Cambridge: Cambridge University Press. pp. 285–356.
Lucey P. G., Taylor G. J., and Malaret E. 1995. Abundance and distribution of iron on the Moon. *Science* 268:1150–1153.
McKay D. S., Bogard D. D., Morris R. V., Korotev R. L., Johnson P., and Wentworth S. J. 1986. Apollo 16 regolith breccias: Characterization and evidence for early formation in the mega-regolith. Proceedings, 16th Lunar and Planetary Science Conference. pp. D277–D303.
McKay D. S., Bogard D. D., Morris R. V., Korotev R. L., Wentworth S. J., and Johnson P. 1989. Apollo 15 regolith breccias: Window to a KREEP regolith. Proceedings, 19th Lunar and Planetary Science Conference. pp. 19–41.
Metzger A. E., Haines E. L., Parker R. E., and Radocinski R. G. 1977. Thorium concentrations in the lunar surface. I. Regional values and crustal content. Proceedings, 8th Lunar Science Conference. pp. 949–999.
Meyer C. 1994. Catalog of Apollo 17 rocks, volume 4, North Massif. JSC #26088. Washingon, D.C.: Government Printing Office. 644 p.
Mittlefehldt D. W. and Hörz F. 1998. Siderophile element fractionation in impact glasses from Meteor Crater (abstract #1771). 29th Lunar and Planetary Science Conference. CD-ROM.
Morris R. V. 1978. The surface exposure (maturity) of lunar soils: Some concepts and Is/FeO compilation. Proceedings, 9th Lunar and Planetary Science Conference. pp. 2287–2297.
Morris R. V., See T. H., and Hörz F. 1986. Composition of the Cayley Formation at Apollo 16 as inferred from impact melt splashes. Proceedings, 17th Lunar and Planetary Science Conference. pp. E21–E42.
Naney M. T., Crowl D. M., and Papike J. J. 1976. The Apollo 16 drill core: Statistical analysis of glass chemistry and the characterization of a high alumina-silica poor (HASP) glass. Proceedings, 7th Lunar Science Conference. pp. 155–184.
Nazarov M. A., Demidova S. I., Patchen A., and Taylor L. A. 2002. Dhofar 301, 30, and 303: Three new lunar highland meteorites from Oman (abstract #1293). 33rd Lunar and Planetary Science Conference. CD-ROM.
Nazarov M. A., Demidova S. I., Patchen A., and Taylor L. A. 2004. Dhofar 311, 730, and 731: New lunar meteorites from Oman (abstract #1233). 35th Lunar and Planetary Science Conference. CD-ROM.
Neumann G. A., Zuber M. T., Smith D. E., and Lemoine F. G. 1996. The lunar crust: Global structure and signature of major basins. *Journal of Geophysical Research* 101:16,841–16,863.
Nishiizumi K. and Caffee M. W. 2001. Exposure histories of lunar meteorites Dhofar 025, 026, and Northwest Africa 482 (abstract). *Meteoritics & Planetary Science* 36:A148–A149.
Nishiizumi K., Caffee M. W., and Jull A. J. T. 1998. Exposure histories of Dar al Gani 262 lunar meteorites (abstract #1957). 29th Lunar and Planetary Science Conference. CD-ROM.
Nishiizumi K., Caffee M. W., Jull A. J. T., and Reedy R. C. 1996. Exposure history of lunar meteorites Queen Alexandra Range 93069 and 94269. *Meteoritics & Planetary Science* 31:893–896.
Nishiizumi K., Hillegonds D. J., McHargue L. R., and Jull A. J. T. 2004. Exposure and terrestrial histories of new lunar and martian meteorites (abstract #1130). 35th Lunar and Planetary Science Conference. CD-ROM.
Nishiizumi K., Okazaki R., Park J., Nagao K., Masarik J., and Finkel R. C. 2002. Exposure and terrestrial histories of Dhofar 019 martian meteorite (abstract #1366). 33rd Lunar and Planetary Science Conference. CD-ROM.
Nord G. L., Jr., Christie J. M., Lally J. S., and Heuer A. H. 1977. The thermal and deformational history of Apollo 15418, a partly shock-melted lunar breccia. *The Moon* 17:217–231.
Polnau E. and Eugster O. 1998. Cosmic-ray-produced, radiogenic, and solar noble gases in lunar meteorites Queen Alexandra Range 94269 and 94281. *Meteoritics & Planetary Science* 33: 313–319.
Ringwood A. E., Seifert S., and Wänke H. 1987. A komatiite component in Apollo 16 highland breccias: Implications for the nickel-cobalt systematics and bulk composition of the Moon. *Earth and Planetary Science Letters* 81:105–117.
Ryder G. 1985. Catalog of Apollo 15 rocks. Curatorial Facility Publication #20787. Washington, D.C.: Government Printing Office. 1296 p.
Ryder G. 1992. Impact melt breccias at the Apollo 17 landing site (abstract). Workshop on the Geology of the Apollo 17 Landing Site. pp. 49–50.
Ryder G. and Norman M. D. 1980. Catalog of Apollo 16 rocks.

Curatorial Branch Publication #52-JSC16904. Washington, D.C.: Government Printing Office. 1144 p.

Scherer P., Pätsch M., and Schultz L. 1998. Noble gas study of the new lunar highland meteorite Dar al Gani 400. *Meteoritics & Planetary Science* 33:A135–A136.

Schnabel C., Ma P., Herzog G. F., Faestermann T., Knie K., and Korschinek G. 2001. ^{10}Be, ^{26}Al, and ^{53}Mn in martian meteorites (abstract #1353). 32nd Lunar and Planetary Science Conference. CD-ROM.

Schultz P. H. 1995. Making the man in the Moon: Origin of the Imbrium Basin (abstract). 26th Lunar and Planetary Science Conference. pp. 1251–1252.

Shearer C. K. and Papike J. J. 1999. Magmatic evolution of the Moon. *American Mineralogist* 84:1469–1494.

Shukolyukov Y. A., Nazarov M. A., Pätsch M., and Schultz L. 2001. Noble gases in three lunar meteorites from Oman (abstract #1502). 32nd Lunar and Planetary Science Conference. CD-ROM.

Simon S. B., Papike J. J., and Laul J. C. 1981. The lunar regolith: Comparative studies of the Apollo and Luna sites. Petrology of soils from Apollo 17, Luna 16, 20, and 24. Proceedings, 12th Lunar and Planetary Science Conference. pp. 371–388.

Simonds C. H., Warner J. L., Phinney W. C., and McGee P. E. 1976. Thermal model for impact breccia lithification: Manicouagan and the Moon. Proceedings, 7th Lunar Science Conference. pp. 2509–2528.

Smith M. R., Schmitt R. A., Warren P. H., Taylor G. J., and Keil K. 1983. Far-eastern nonmare samples: New data from Luna 20 and 16 (abstract). 14th Lunar and Planetary Science Conference. p. 716.

Snyder G. A., Taylor L. A., Patchen A., Nazarov M. A., and Semenova T. S. 1999. Mineralogy and petrology of a primitive spinel troctolite and gabbros from Luna 20, eastern highlands of the Moon (abstract #1491). 30th Lunar and Planetary Science Conference. CD-ROM.

Spettel B., Dreibus G., Burghele A., Jochum K. P., Schultz L., Weber H. W., Wlotzka F., and Wänke H. 1995. Chemistry, petrology, and noble gases of lunar highland meteorite Queen Alexandra Range 93069. *Meteoritics & Planetary Science* 30:581–582.

Stöffler D., Knöll H.-D., Marvin U. B., Simonds C. H., and Warren P. H. 1980. Recommended classification and nomenclature of lunar highland rocks: A committee report. In *Proceedings of the conference on the lunar highlands crust*, edited by Merrill R. B. and Papike J. J. New York: Pergamon Press. pp. 51–70.

Swindle T. 1995. Noble gases in the lunar meteorites Calcalong Creek and Queen Alexandra Range 93069. *Meteoritics & Planetary Science* 30:584–585.

Swindle T. D., Spudis P. D., Taylor G. J., Korotev R. L., Nichols R. H., Jr., and Olinger C. T. 1991. Searching for Crisium Basin ejecta: Chemistry and ages of Luna 20 impact melts. Proceedings, 21st Lunar and Planetary Science Conference. pp. 167–181.

Symes S. J. K., Sears D. W. G., Akridge D. G., Huang S., and Benoit P. H. 1998. The crystalline lunar spherules: Their formation and implications for the origin of meteoritic chondrules. *Meteoritics & Planetary Science* 33:13–29.

Takeda H., Miyamoto M., Mori H., Wentworth S. J., and McKay D. S. 1990. Mineralogical comparison of the Y-86032-type lunar meteorites to feldspathic fragmental breccia 67016. Proceedings, 20th Lunar and Planetary Science Conference. pp. 91–100.

Takeda H., Bogard D. D., Yamaguchi A., Ohtake M., and Saiki K. 2004. A crustal rock clast in magnesian anorthositic breccia, Dhofar 489 and its excavation from a large basin (abstract #1222). 35th Lunar and Planetary Science Conference. CD-ROM.

Taylor L. A., Nazarov M. A., Cohen B. A., Warren P. H., Barsukova L. D., Clayton R. N., and Mayeda T. K. 2001. Bulk chemistry and oxygen isotopic compositions of lunar meteorites Dhofar 025 and Dhofar 026 (abstract #1985). 32nd Lunar and Planetary Science Conference. CD-ROM.

Thalmann C., Eugster O., Herzog G. F., Klein J., Krähenbühl U., Vogt S., and Xue S. 1996. History of lunar meteorites Queen Alexandra Range 93069, Asuka-881757, and Yamato-791639 based on noble gas abundances, radionuclide concentrations, and chemical composition. *Meteoritics & Planetary Science* 31:857–868.

Walker R. J., Horan M. F., Shearer C. K., and Papike J. J. 2004. Low abundances of highly siderophile elements in the lunar mantle: Evidence for prolonged late accretion (abstract #1110). 35th Lunar and Planetary Science Conference. CD-ROM.

Wänke H., Baddenhausen H., Balacescu A., Teschke F., Spettel B., Dreibus G., Palme H., Quijano-Rico M., Kruse H., Wlotzka F., and Begemann F. 1972. Multielement analyses of lunar samples and some implications of the results. Proceedings, 3rd Lunar Science Conference. pp. 1251–1268.

Wark D. A. 1987. Plagioclase-rich inclusions in carbonaceous chondrite meteorites: Liquid condensates? *Geochimica et Cosmochimica Acta* 51:221–242.

Warren P. H. 1988. The origin of pristine KREEP: Effects of mixing between urKREEP and the magmas parental to the Mg-rich cumulates. Proceedings, 18th Lunar and Planetary Science Conference. pp. 233–241.

Warren P. H. 1990. Lunar anorthosites and the magma ocean hypothesis: Importance of FeO enrichment in the parent magma. *American Mineralogist* 75:46–58.

Warren P. H. 1994. Lunar and martian meteorite delivery services. *Icarus* 111:338–363.

Warren P. H. 2001. Porosities of lunar meteorites: Strength, porosity, and petrologic screening during the meteorite delivery process. *Journal of Geophysical Research* 106:10,101–10,112.

Warren P. H. 2004. The Moon. In *Treatise on geochemistry*, volume 1, edited by Davis A. M. San Diego: Elsevier. pp. 559–599.

Warren P. H. 2005. "New" lunar meteorites: Implications for composition of the global lunar surface, of the lunar crust, and the bulk Moon. *Meteoritics & Planetary Science* 40:477–506.

Warren P. H. and Bridges J. C. 2004. Lunar meteorite Yamato-983885: A relatively KREEPy regolith breccia, not paired with Y-791197 (abstract). *Meteoritics & Planetary Science* 39:A112.

Warren P. H. and Kallemeyn G. W. 1984. Pristine rocks (8th foray): "Plagiophile" element ratios, crustal genesis, and the bulk composition of the Moon. Proceedings, 15th Lunar and Planetary Science Conference. pp. C16–C24.

Warren P. H. and Kallemeyn G. W. 1991. The MacAlpine Hills lunar meteorite, and implications of the lunar meteorites collectively for the composition and origin of the Moon. *Geochimica et Cosmochimica Acta* 55:3123–3138.

Warren P. H. and Kallemeyn G. W. 2001. New lunar meteorite Northwest Africa 482: An anorthositic impact melt breccia with low KREEP content (abstract). *Meteoritics & Planetary Science* 36:A220.

Warren P. H. and Wasson J. T. 1978. Compositional-petrographic investigation of pristine nonmare rocks. Proceedings, 9th Lunar and Planetary Science Conference. pp. 185–217.

Warren P. H. and Wasson J. T. 1980a. Early lunar petrogenesis, oceanic and extraoceanic. *Proceedings of the conference on the lunar highlands crust*, edited by Merrill R. B. and Papike J. J. New York: Pergamon Press. pp. 81–99.

Warren P. H. and Wasson J. T. 1980b. Further foraging for pristine nonmare rocks: Correlations between geochemistry and longitude. Proceedings, 11th Lunar Science Conference. pp. 431–470.

Warren P. H., Jerde E. A., and Kallemeyn G. W. 1989. Lunar meteorites: Siderophile element contents, and implications for the composition and origin of the Moon. *Earth and Planetary Science Letters* 91:245–260.

Warren P. H., Kallemeyn G. W., and Kyte F. T. 1999. Origin of planetary cores: Evidence from highly siderophile elements in martian meteorites. *Geochimica et Cosmochimica Acta* 63:2105–2122.

Warren P. H., Taylor G. J., and Keil K. 1983. Regolith breccia Allan Hills A81005: Evidence of lunar origin, and petrography of pristine and nonpristine clasts. *Geophysical Research Letters* 10: 779–782.

Wasson J. T. and Kallemeyn G. W. 1988. Compositions of chondrites. *Philosophical Transactions of the Royal Society of London A* 325:535–544.

Wasson J. T., Boynton W. V., Chou C.-L., and Baedecker P. A. 1975. Compositional evidence regarding the influx of interplanetary materials onto the lunar surface. *The Moon* 13:121–141.

Wieczorek M. A. and Phillips R. J. 2000. The "Procellarum KREEP Terrane": Implications for mare volcanism and lunar evolution. *Journal of Geophysical Research* 105:20,417–20,430.

Yanai K. and Kojima H. 1987. *Photographic catalog of the Antarctic meteorites*. Tokyo: National Institute of Polar Research. 298 p.

Zipfel J., Spettel B., Palme H., Wolf D., Franchi I., Sexton A. S., Pillinger C. T., and Bischoff A. 1998. Dar al Gani 400: Chemistry and petrology of the largest lunar meteorite (abstract). *Meteoritics & Planetary Science* 33:A171.